REFERENCES

1. Hsu, B. Y.; Cheng. S. Pinacol rearrangement over metal-substituted aluminophosphate molecular sieves. *Microporous and Mesoporous Mater.* 21 (1998): 5005-5015.

2. Hsien, M.; Sheu, H.-T.; Lee, T.; Cheng, S.; Lee, J.-F. Fe-substituted molecular sieves as catalysts in liquid phase pinacol rearrangement. *J. Mol. Catal. A* 181 (2002): 189-200.

3. Nakamura, K.; Osamura, Y. Theoretical study of the reaction mechanism and migratory aptitude of the pinacol rearrangement., *J. Am. Chem. Soc.* 115 (1993): 9112-9120.

4. Lezaeta, M. D.; Sattar, W.; Svoronos, P.; Karimia, S.; Subramaniamb, G. Effect of various acids at different concentrations on the pinacol rearrangement. *Tetrahedron Lett.* 43 (2002): 9307- 9309.

5. Bezouhanova, C.P.; Jabur, F.A.; Zeolite catalysts for pinacol rearrangement. *J. Mol. Catal.* 87 (1994): 39-46.

6. Bucsi, I.; Molnár, A.; Bartók, M.; Olah, G.A. Transformation of 1, 2-diols over perfluorinated resinsulfonic acids (Nafion-H). *Tetrahedron* 50 (1994): 8195-8202.

7. Campelo, J. M.; R.; Chakraborty, Marinas, J. M.; Romero, A. A. Gas-phase pinacol conversion on $AlPO_4$, Al_2O_3 and SiO_2 catalysts. *Catal. Lett.* 54 (1998): 91-93.

8. Török, B.; Bucsi, I.; Beregszászi, T.; Kapocsi, I.; Molnár, A. Transformation of diols in the presence of heteropoly acids under homogeneous and heterogeneous conditions. *J. Mol. Catal. A* 107 (1996): 305-311.

9. Ranjbar, P. R.; Kianmehr, E. Facile and fast pinacol rearrangement by $AlCl_3$ in the solid state. *Molecules* 6 (2001): 442-447.

10. Loeser, E.; Chen, G-P.; He, T.; Prasad, K.; Repic, O. Mechanism of the pinacol–pinacolone rearrangement of 2,3-di-(3-pyridyl)-2,3-butanediol in sulfuric acid. *Tetrahedron Lett.* 43 (2002): 2161-2165.

11. Chatterjee, A.; Chandra, A. K. Fe and B substitution in ZSM-5 zeolites: a quantum mechanical study. *J. Mol. Catal. A* 119 (1997): 5l-56.

12   Szostak, R. *Molecular sieves: principles of sythesis and identification*. New York: Van Nostand Reinhold, (1989).

13.   Weitkamp, J. Zeolites and catalysis. *Solid State Ionics* 131 (2000): 175-188.

14.   Corma, A. Inorganic solid acids and their use in acid-catalyzed hydrocarbon reactions. *Chem. Rev.* 95 (1995): 559-614.

15.   van Santen, R. A.; Kramer, G. J. Reactivity theory of zeolitic Brønsted acidic sites. *Chem. Rev.* 95 (1995): 637-660.

16.   Ghobarbar, H.; Schäf, O.; Guth, U. Zeolite from kitchen to space. *Prog. Solid St. Chem.* 27 (1999): 29-73.

17.   Sen, S. E.; Smith, S. M.; Sullivan, K. A. Organic transformations using zeolite and zeotype materials. *Tetrahedron* 55 (1999): 12657-12698.

18.   Kindler, J.; Geidel, E.; Förster, H. Application of density functional hybrid of zeolites methods to cluster models. *Solid State Ionics* 101-103 (1997): 825-832.

19.   Dyer, A. *An introduction to zeolite molecular sieves*. New York: John Wiley & Sons, (1988).

20.   Blaszkowski, R. S.; van Santen, A. R. Quantum chemical studies of zeolite proton catalyzed reaction. *Topics in Catalysi*s 4 (1997): 145-156.

21.   Fermann, T. J.; Blanco, C. Modeling proton mobility in acidic zeolite clusters. I. Convergence of transition state parameters from quantum chemistry. *J. Chem. Phys.* 112 (2000): 6779-6786.

22.   Sillar, K.; Burk, P. Hybrid quantum chemical and density functional theory (ONIOM) study of the acid sites in zeolite ZSM-5. *J. Phys. Chem. B* 108 (2004): 9893-9899.

23.   Zygmunt, A. S.; Muller, M. R.; Curtiss, A. L.; Iton, E. L. An assessment of density dunctional methods for studying molecular adsorption in cluster models of zeolites. *J. Mol. Struct. (Theochem)* 430 (1998): 9-16.

24.   Fărcaşiu, D.; Lukinskas, P. Mechanism and reactivity of alkane C-H bond dissociation on coordinatively unsaturated aluminum ions, determined by theoretical calculations. *J. Phys. Chem. A* 106 (2002): 1619-1626.

25.   Bezouhanova, P. C.; Jabur, A. F. Zeolite catalysts for pinacol rearrangement. *J. Mol. Catal.* 87, (1994): 39-46.

26. Solans-Monfort, X.; Bertran, J.; Branchadell, V.; Sodupe, M. Keto-enol isomerization of acetaldehyde in HZSM5. A theoretical study using the ONIOM2 method. *J. Phys. Chem. B* 106 (2002): 10220-10226.

27. Bordiga, S.; Coluccia, S.; Lamberti, C.; Marchese, L.; Zecchina,A.; Boscherini, F.; Buffa, F.; Genoni, F.; Leofanti, G.; Vlaic, G. XAFS study of Ti-silicalite: structure of framework Ti(IV) in the presence and absence of reactive molecules (H_2O, NH_3) and comparison with ultraviolet-visible and IR results. *J. Phys. Chem.* 98 (1994): 4125-4132.

28. Fricke, R.; Kosslick, H.; Lischke, G.; Richter, M. Incorporation of gallium into zeolites: syntheses, properties and catalytic application. *Chem. Rev.* 100 (2000): 2303-2406.

29. Yoshizawa, K.; Yumura, T.; Shiota, Y.; Yamabe, T. Formation of an Iron-oxo species upon decomposition of dinitrogen oxide on a model of Fe-ZSM5 zeolite. *Bull. Chem. Soc. Jpn.* 73 (2000): 29-36.

30. Dong, M.; Wang, J.; Sun, Y. Synthesis of zincosilicate mordenite using citric acid as complexing agent. *Microporous Mesoporous Mater.* 43 (2001): 237-243.

31. Yuan, S. P.; Wang, J. G.; Li, Y. W.; Jiao, H. Brønsted acidity of isomorphously substituted ZSM-5 by B, Al, Ga, and Fe. Density functional investigations. *J. Phys. Chem. A* 106 (2002): 8167-8172.

32. Yoshizawa, K.; Shiota, Y.; Yumura, T.; Yamabe, T. Direct methane-methanol and benzene-phenol conversions on Fe-ZSM-5 zeolite: theoretical predictions on the reaction pathways and energetics. *J. Phys. Chem. B* 104 (2000): 734-740.

33. Kachurovskaya, N. A.; Zhidomirov, G. M.; Hensen, E. J.M.; van Santen, R. A. Cluster model DFT study of the intermediates of benzene to phenol oxidation by N_2O on FeZSM-5 zeolites. *Catal. Lett.* 86 (2003): 25-31.

34. Yoshizawa, K.; Shiota, Y.; Kamachi, T. Mechanistic proposals for direct benzene hydroxylation over Fe-ZSM-5 zeolite. *J. Phys. Chem. B* 107 (2003): 11404-11410.

35. Kachurovskaya, N. A.; Zhidomirov, G. M.; van Santen R. A. Computational study of benzene-to-phenol oxidation catalyzed by N_2O on iron-exchanged ferrierite. *J. Phys. Chem. B* 108 (2004): 5944-5950.

36. Kumar, M. S.; Schwidder, M.; Grünert, W.; Brückner, A. On the nature of different iron sites and their catalytic role in Fe-ZSM-5 deNO$_x$ catalysts: new insights by a combined EPR and UV/VIS spectroscopic approach. *J. Catal.* 227 (2004): 384-397.

37. Yakoviev, A. L.; Zhidomirov, G. M.; van Santen R. A. DFT calculations on N$_2$O decomposition by binuclear Fe complexes in Fe/ZSM-5. *J. Phys. Chem. B* 105 (2001): 12297-12302.

38. Yuan, S. P.; Wanga,, J. G.; Lia, Y. W.; Jiao, H. Density functional investigations into the siting of Fe and the acidic properties of isomorphously substituted mordenite by B, Al, Ga and Fe. *J. Mol. Struct. (Theochem)* 674 (2004): 267-274.

39. Villa, A.L.; Caro, C. A.; de Correa, C. M. Cu- and Fe-ZSM-5 as catalysts for phenol hydroxylation. *J. Mol. Catal. A* 228 (2005): 233–240.

40. Liese, T.; Grünert, W. Cu–Na–ZSM-5 catalysts prepared by chemical transport: investigations on the role of Brønsted acidity and of excess Copper in the selective catalytic reduction of NO by propene. *J. Catal.* 172 (1997): 34-45.

41. de Carvalho, M. C. N. A.; Passos, F. B.; Schmal, M. The behavior of Cu/ZSM-5 in the oxide and reduced form in the presence of NO and methanol. *Appl. Catal. A* 193 (2000): 265-276.

42. Sierraalta, A.; Bermudeza, A.; Brussinb, M. R. Density functional study of the interaction of Cu$^{\tau}$ ion-exchanged zeolites with H$_2$O and SO$_2$ molecules. *J. Mol. Catal. A* 228 (2005): 203-210.

43. Kanougi, T.; Tsuruya, H.; Oumi, Y.; Chatterjee, A.; Fahmi, A.; Kubo, M.; Miyamoto, A. Density functional calculation on the adsorption of nitrogen oxides and water on ion exchanged ZSM-5. *App. Surf. Sci.* 130–132 (1998): 561-565.

44. Liang, W.; Bell, A. T.; Head-Gordon, M.; Chakraborty, A. K. Density functional theory investigations of the direct oxidation of methane on an Fe-exchanged zeolite. *J. Phys. Chem. B* 108 (2004): 4362-4368.

45. Kita, Y.; Yoshida, Y.; Mihara, S.; Furukawa, A.; Higuchi, K.; Fang, D-F.; Fujioka, H. Non-dehydrative pinacol rearrangement using a Lewis acid-trialkyl orthoester combined system. *Tetrahedron* 54 (1998): 14689-14704.

46. Smith, B. W. Ethylene glycol to acetaldehyde-dehydration or a concerted mechanism. *Tetrahedron* 58 (2002): 2091-2094.

47. Dai, Z.; Hatano, B.; Tagaya, H. Catalytic dehydration of propylene glycol with salts in near-critical water. *App. Catal. A* 258 (2004): 189-193.

48. Pachuau, Z.; Lyngdoh, D. R. Molecular orbital studies on the Wagner-Meerwein migration in some acyclic pinacol–pinacolone rearrangements. *J. Chem. Sci.* 116 (2004): 83-91.

49. Simons, J. *An introduction to theoretical chemistry.* Cambridge: Cambridge University Press, (2003).

50. Jensen, F. *Introduction to computational chemistry.* Chichester: John Wiley & Sons, (1999).

51. Hammond, S.G. A Correlation of Reaction Rates. *J. Am. Chem. Soc.* 77 (1955): 334-338.

52. Donahue, M. N. Revisiting the Hammond postulate: the role of reactant and product ionic states in regulating barrier heights, locations, and transition state frequencies. *J. Phys. Chem. A* 105 (2001): 1489-1497.

53. Adam, W.; Bach, R.D; Dmitrenko, O.; Saha-Möller, C.R. A computational study of the hydroxy-group directivity in the peroxyformic scid epoxidation of the chiral allylic alcohol (*Z*)-3-methyl-3-penten-2-ol: control of threo diastereoselectivity through allylic strain and hydrogen bonding. *J. Org. Chem.* 65 (2000): 6715-6728.

APPENDICES

APPENDIX A

Figure A1 Relative energetic profiles of propylene glycol in pinacol rearrangement in non-catalyst system (neutral water) of model I.
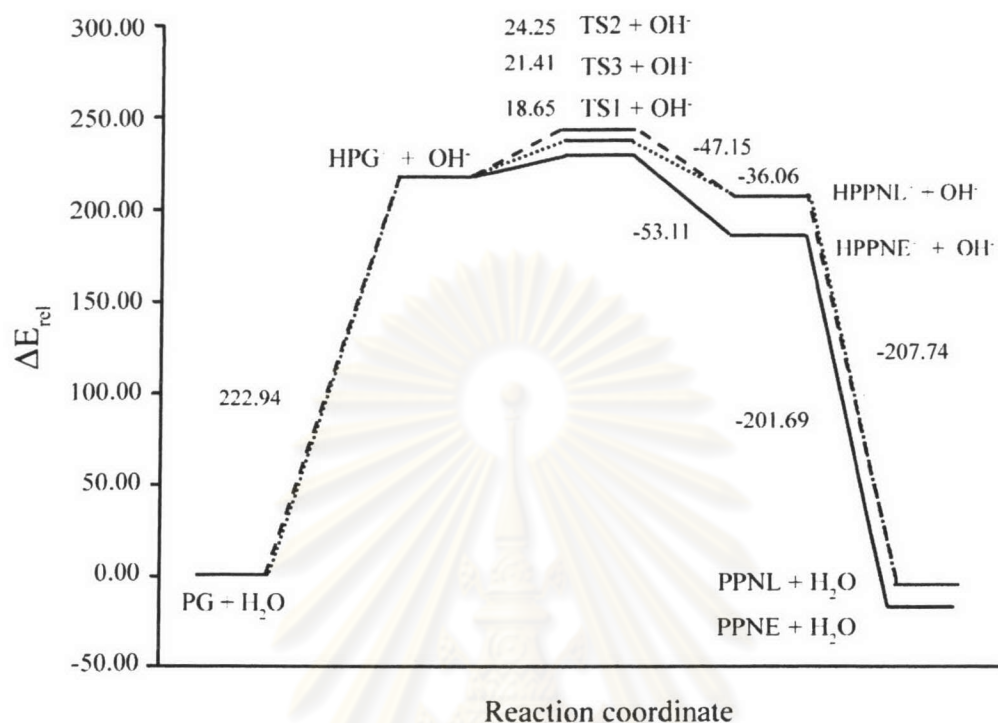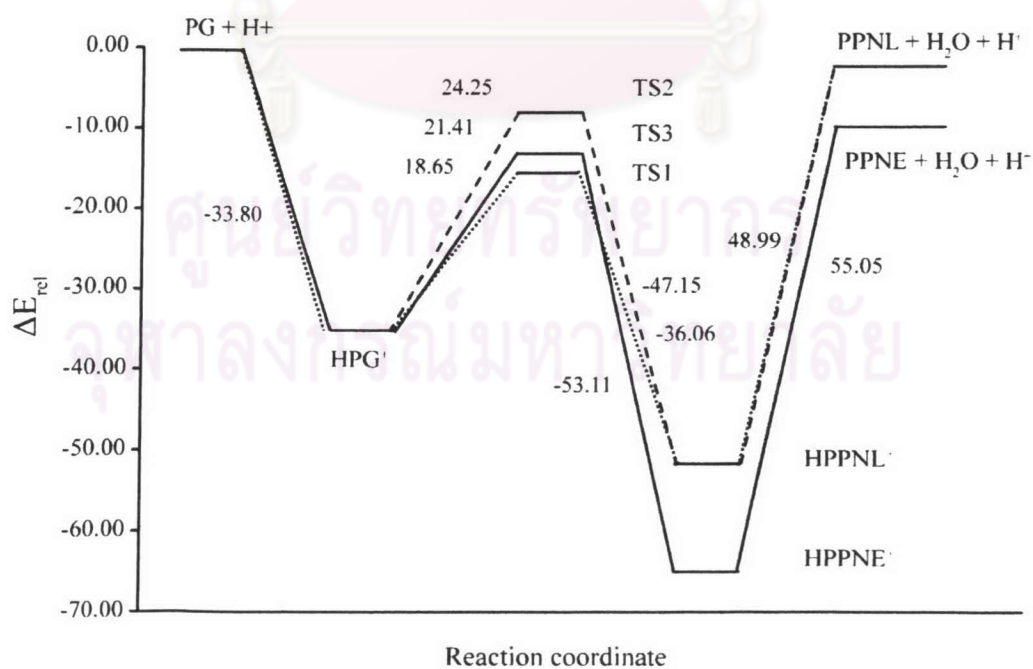

Figure A2 Relative energetic profiles of propylene glycol in pinacol rearrangement in acid-catalyst system of model I.
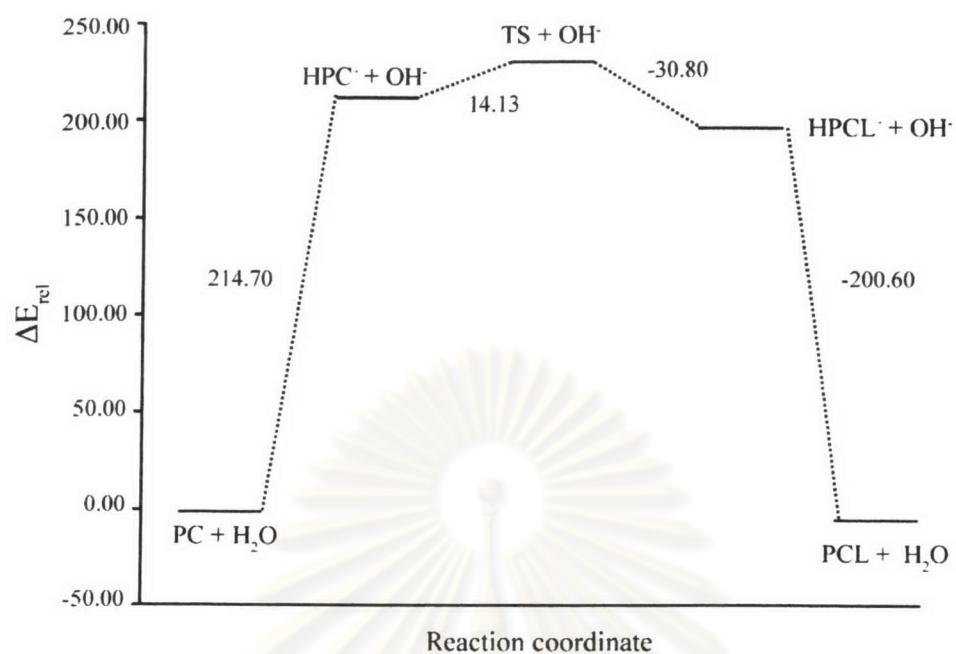
Figure A3 Relative energetic profiles of pinacol rearrangement in non-catalyst system (neutral water).
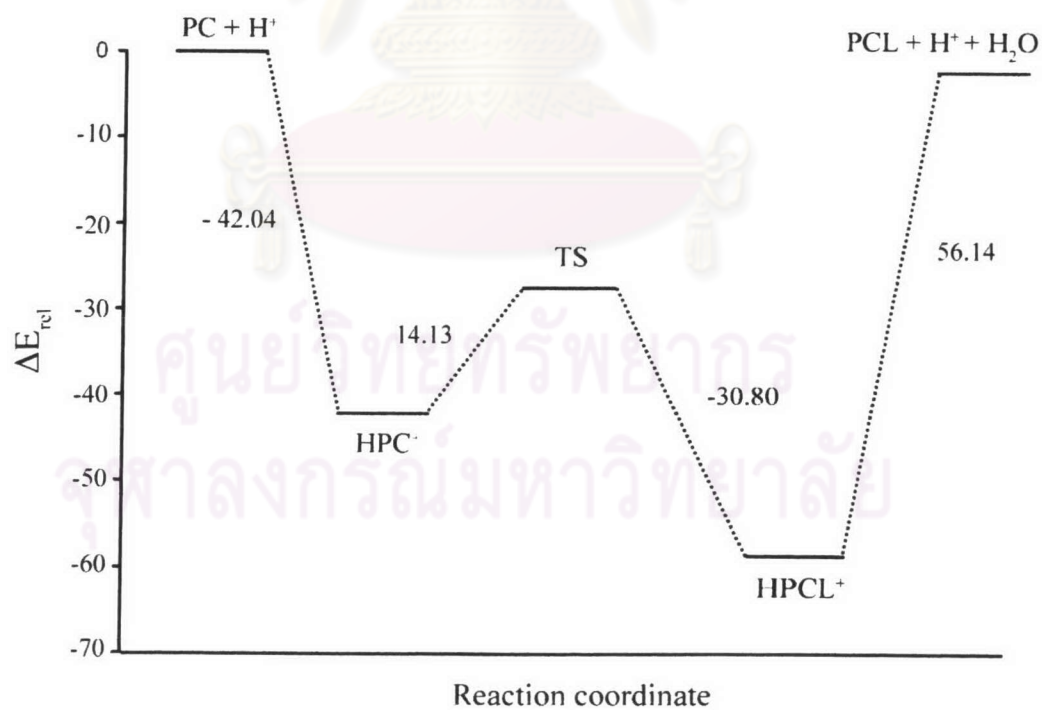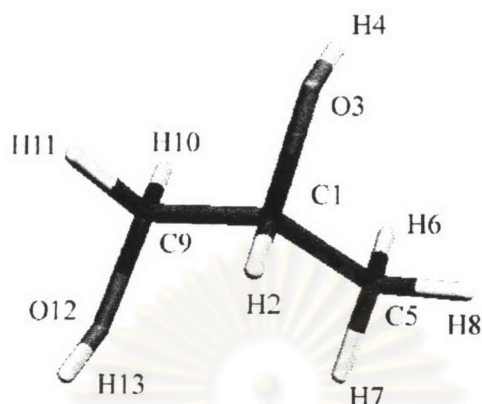

Figure A4 Relative energetic profiles of pinacol rearrangement in acid-catalyst system.

APPENDIX B

Table B1 Geometrical parameters of propylene glycol.

Bond Length	Value (Angstroms)	Angle	Value (Degrees)	Dihedral	Value (Degrees)
R(1,2)	1.0989	A(2,1,3)	104.3756	D(2,1,3,4)	172.2819
R(1,3)	1.4284	A(2,1,5)	109.2252	D(5,1,3,4)	54.0951
R(1,5)	1.5259	A(2,1,9)	108.2548	D(9,1,3,4)	-71.9019
R(1,9)	1.5367	A(3,1,5)	112.2779	D(2,1,5,6)	64.496
R(3,4)	0.9711	A(3,1,9)	109.734	D(2,1,5,7)	-176.6713
R(5,6)	1.0943	A(5,1,9)	112.577	D(2,1,5,8)	-56.7723
R(5,7)	1.0994	A(1,3,4)	107.2492	D(3,1,5,6)	179.7746
R(5,8)	1.0945	A(1,5,6)	110.6041	D(3,1,5,7)	-61.3927
R(9,10)	1.0976	A(1,5,7)	110.3953	D(3,1,5,8)	58.5063
R(9,11)	1.1001	A(1,5,8)	110.7366	D(9,1,5,6)	-55.7873
R(9,12)	1.4232	A(6,5,7)	107.4858	D(9,1,5,7)	63.0454
R(12,13)	0.9699	A(6,5,8)	109.2548	D(9,1,5,8)	-177.0555
		A(7,5,8)	108.2742	D(2,1,9,10)	-179.4897
		A(1,9,10)	109.4493	D(2,1,9,11)	63.2927
		A(1,9,11)	108.7902	D(2,1,9,12)	-61.9009
		A(1,9,12)	113.2617	D(3,1,9,10)	67.1777
		A(10,9,11)	107.5198	D(3,1,9,11)	-50.04
		A(10,9,12)	105.6461	D(3,1,9,12)	-175.2336
		A(11,9,12)	111.9663	D(5,1,9,10)	-58.6489
				D(5,1,9,11)	-175.8665
				D(5,1,9,12)	58.9399
				D(1,9,12,13)	69.4236
				D(10,9,12,13)	-170.7894
				D(11,9,12,13)	-54.042

Propanal

Propanone
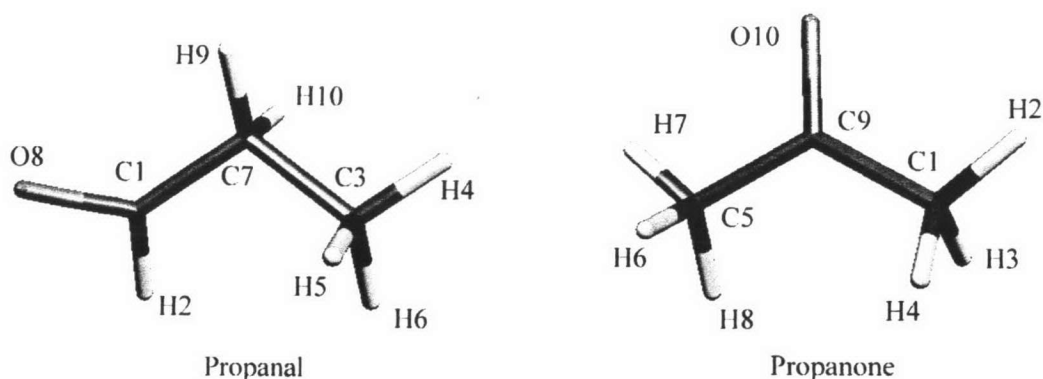
Table B2 Geometrical parameters of propanal

Bond Length	Value (Angstroms)	Angle	Value (Degrees)	Dihedral	Value (Degrees)
R(1,2)	1.1161	A(2,1,7)	114.404	D(2,1,7,3)	53.256
R(1,7)	1.5126	A(2,1,8)	120.5082	D(2,1,7,9)	177.1784
R(1,8)	1.2107	A(7,1,8)	125.0874	D(2,1,7,10)	-66.5402
R(3,4)	1.0953	A(4,3,5)	107.95	D(8,1,7,3)	-126.5227
R(3,5)	1.0944	A(4,3,6)	107.8837	D(8,1,7,9)	-2.6003
R(3,6)	1.0965	A(4,3,7)	111.1752	D(8,1,7,10)	113.6811
R(3,7)	1.5375	A(5,3,6)	107.726	D(4,3,7,1)	64.1548
R(7,9)	1.0945	A(5,3,7)	110.6431	D(4,3,7,9)	-57.8002
R(7,10)	1.1009	A(6,3,7)	111.3141	D(4,3,7,10)	-177.1378
		A(1,7,3)	111.9493	D(5,3,7,1)	-175.9038
		A(1,7,9)	108.4259	D(5,3,7,9)	62.1412
		A(1,7,10)	107.335	D(5,3,7,10)	-57.1964
		A(3,7,9)	111.8968	D(6,3,7,1)	-56.1528
		A(3,7,10)	109.1833	D(6,3,7,9)	-178.1078
		A(9,7,10)	107.8678	D(6,3,7,10)	62.5546

Table B3 Geometrical parameters of propanone.

Bond Length	Value (Angstroms)	Angle	Value (Degrees)	Dihedral	Value (Degrees)
R(1,2)	1.0917	A(2,1,3)	109.5799	D(2,1,9,5)	179.9219
R(1,3)	1.0974	A(2,1,4)	109.557	D(2,1,9,10)	-0.1052
R(1,4)	1.0974	A(2,1,9)	109.8452	D(3,1,9,5)	58.8892
R(1,9)	1.5206	A(3,1,4)	106.794	D(3,1,9,10)	-121.1379
R(5,6)	1.0974	A(3,1,9)	110.5228	D(4,1,9,5)	-59.0952
R(5,7)	1.0917	A(4,1,9)	110.4899	D(4,1,9,10)	120.8777
R(5,8)	1.0974	A(6,5,7)	109.557	D(6,5,9,1)	59.0952
R(5,9)	1.5206	A(6,5,8)	106.794	D(6,5,9,10)	-120.8777
R(9,10)	1.2157	A(6,5,9)	110.4899	D(7,5,9,1)	-179.9219
		A(7,5,8)	109.5799	D(7,5,9,10)	0.1052
		A(7,5,9)	109.8452	D(8,5,9,1)	-58.8892
		A(8,5,9)	110.5228	D(8,5,9,10)	121.1379
		A(1,9,5)	116.5008		
		A(1,9,10)	121.7496		
		A(5,9,10)	121.7496		
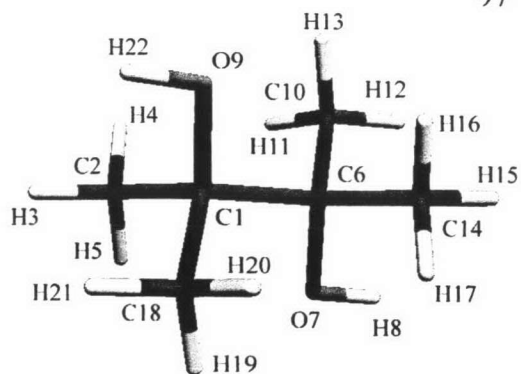
Table B4 Geometrical parameters of pinacol.

Bond Length	Value (Angstroms)	Angle	Value (Degrees)	Dihedral	Value (Degrees)
R(1,2)	1.5375	A(2,1,6)	111.596	D(6,1,2,3)	-178.1109
R(1,6)	1.5663	A(2,1,9)	108.8824	D(6,1,2,4)	-58.2306
R(1,9)	1.4378	A(2,1,18)	110.087	D(6,1,2,5)	63.0694
R(1,18)	1.5393	A(6,1,9)	105.2668	D(9,1,2,3)	-62.3452
R(2,3)	1.0986	A(6,1,18)	112.2544	D(9,1,2,4)	57.5351
R(2,4)	1.0908	A(9,1,18)	108.5549	D(9,1,2,5)	178.8351
R(2,5)	1.0949	A(1,2,3)	109.441	D(18,1,2,3)	56.5475
R(6,7)	1.4378	A(1,2,4)	110.1572	D(18,1,2,4)	176.4278
R(6,10)	1.5393	A(1,2,5)	112.2764	D(18,1,2,5)	-62.2722
R(6,14)	1.5375	A(3,2,4)	109.0454	D(2,1,6,7)	45.882
R(7,8)	0.9699	A(3,2,5)	107.126	D(2,1,6,10)	-72.0284
R(9,22)	0.9699	A(4,2,5)	108.7035	D(2,1,6,14)	163.8408
R(10,11)	1.0941	A(1,6,7)	105.2668	D(9,1,6,7)	-72.0767
R(10,12)	1.0972	A(1,6,10)	112.2544	D(9,1,6,10)	170.0129
R(10,13)	1.0947	A(1,6,14)	111.596	D(9,1,6,14)	45.882
R(14,15)	1.0986	A(7,6,10)	108.5549	D(18,1,6,7)	170.0129
R(14,16)	1.0908	A(7,6,14)	108.8824	D(18,1,6,10)	52.1025
R(14,17)	1.0949	A(10,6,14)	110.087	D(18,1,6,14)	-72.0284
R(18,19)	1.0947	A(6,7,8)	106.9975	D(2,1,9,22)	50.8448
R(18,20)	1.0941	A(1,9,22)	106.9975	D(6,1,9,22)	170.6187
R(18,21)	1.0972	A(6,10,11)	111.5146	D(18,1,9,22)	-69.0024
		A(6,10,12)	109.0833	D(2,1,18,19)	57.7397
		A(6,10,13)	112.44	D(2,1,18,20)	-179.7531
		A(11,10,12)	107.5103	D(2,1,18,21)	-61.1595
		A(11,10,13)	108.7909	D(6,1,18,19)	-67.2256
		A(12,10,13)	107.2973	D(6,1,18,20)	55.2817
		A(6,14,15)	109.441	D(6,1,18,21)	173.8753
		A(6,14,16)	110.1572	D(9,1,18,19)	176.8326
		A(6,14,17)	112.2764	D(9,1,18,20)	-60.6601
		A(15,14,16)	109.0454	D(9,1,18,21)	57.9335
		A(15,14,17)	107.126	D(1,6,7,8)	170.6187
		A(16,14,17)	108.7035	D(10,6,7,8)	-69.0024
		A(1,18,19)	112.44	D(14,6,7,8)	50.8448
		A(1,18,20)	111.5146	D(1,6,10,11)	55.2817
		A(1,18,21)	109.0833	D(1,6,10,12)	173.8753
		A(19,18,20)	108.7909	D(1,6,10,13)	-67.2256
		A(19,18,21)	107.2973	D(7,6,10,11)	-60.6601
		A(20,18,21)	107.5103	D(7,6,10,12)	57.9335
				D(7,6,10,13)	176.8326

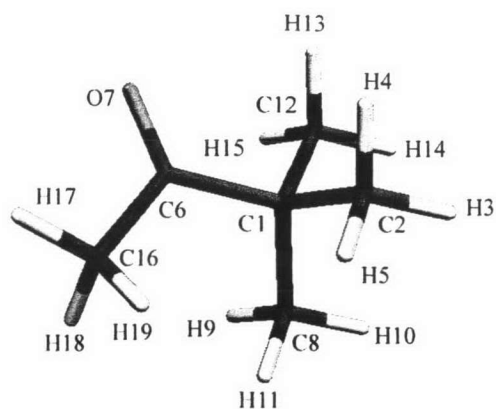**Table B5** Geometrical parameters of pinacolone.

Bond Length	Value (Angstroms)	Angle	Value (Degrees)	Dihedral	Value (Degrees)
R(1,2)	1.5487	A(2,1,6)	107.5781	D(6,1,2,3)	-178.353
R(1,6)	1.5449	A(2,1,8)	109.5485	D(6,1,2,4)	-59.0854
R(1,8)	1.5432	A(2,1,12)	109.4432	D(6,1,2,5)	62.1357
R(1,12)	1.5369	A(6,1,8)	110.8839	D(8,1,2,3)	61.0302
R(2,3)	1.0964	A(6,1,12)	109.3493	D(8,1,2,4)	-179.7022
R(2,4)	1.0957	A(8,1,12)	109.9936	D(8,1,2,5)	-58.4811
R(2,5)	1.0957	A(1,2,3)	109.7328	D(12,1,2,3)	-59.6412
R(6,7)	1.2173	A(1,2,4)	111.0694	D(12,1,2,4)	59.6264
R(6,16)	1.5237	A(1,2,5)	112.1777	D(12,1,2,5)	-179.1525
R(8,9)	1.0967	A(3,2,4)	107.9409	D(2,1,6,7)	104.0075
R(8,10)	1.0963	A(3,2,5)	107.5727	D(2,1,6,16)	-75.5275
R(8,11)	1.0953	A(4,2,5)	108.1919	D(8,1,6,7)	-136.2209
R(12,13)	1.0929	A(1,6,7)	121.2467	D(8,1,6,16)	44.2441
R(12,14)	1.0962	A(1,6,16)	118.7	D(12,1,6,7)	-14.7646
R(12,15)	1.0952	A(7,6,16)	120.0516	D(12,1,6,16)	165.7004
R(16,17)	1.0919	A(1,8,9)	111.4262	D(2,1,8,9)	178.2687
R(16,18)	1.0974	A(1,8,10)	109.794	D(2,1,8,10)	-62.6782
R(16,19)	1.0949	A(1,8,11)	112.2883	D(2,1,8,11)	56.816
		A(9,8,10)	107.5563	D(6,1,8,9)	59.6821
		A(9,8,11)	108.1131	D(6,1,8,10)	178.7352
		A(10,8,11)	107.4697	D(6,1,8,11)	-61.7705
		A(1,12,13)	111.1088	D(12,1,8,9)	-61.3948
		A(1,12,14)	110.1116	D(12,1,8,10)	57.6583
		A(1,12,15)	111.1301	D(12,1,8,11)	177.1526
		A(13,12,14)	108.7329	D(2,1,12,13)	-60.554
		A(13,12,15)	107.386	D(2,1,12,14)	59.9749
		A(14,12,15)	108.2685	D(2,1,12,15)	179.9355
		A(6,16,17)	108.9146	D(6,1,12,13)	57.053
		A(6,16,18)	109.6639	D(6,1,12,14)	177.5818
		A(6,16,19)	112.7066	D(6,1,12,15)	-62.4575
		A(17,16,18)	108.4882	D(8,1,12,13)	179.0459
		A(17,16,19)	109.9334	D(8,1,12,14)	-60.4253
		A(18,16,19)	107.0432	D(8,1,12,15)	59.5354
				D(1,6,16,17)	164.2334
				D(1,6,16,18)	-77.1846
				D(1,6,16,19)	41.9538
				D(7,6,16,17)	-15.3073
				D(7,6,16,18)	103.2746
				D(7,6,16,19)	-137.587

APPENDIX C

Table C1 Cartesian coordinates of C1H transition state of propylene glycol in pinacol rearrangement over 3T cluster model.

Atomic Type	Coordinate (Angstroms)		
	X	Y	Z
O	1.16608600	-1.24715500	-0.06196100
Al	1.28274000	0.37425900	0.72131500
O	0.00965300	1.36802500	-0.10844800
O	0.89789600	0.10092800	2.39658600
O	2.77782600	1.14706200	0.25845600
H	3.55898700	1.00772600	0.80687400
H	0.86791000	0.86333700	2.98737300
Si	2.40100400	-2.06069600	-0.79807000
H	2.80501000	-1.45160700	-2.09512600
H	3.61221700	-2.20091900	0.05649000
H	1.90163200	-3.44069800	-1.09985000
Si	0.27504600	2.76938000	-0.96355000
H	1.16865300	2.55976900	-2.13232600
H	-1.05434300	3.21007300	-1.48975700
H	0.81160300	3.87144600	-0.12136400
C	-2.03315200	-0.91580000	-0.97485100
O	-2.42526300	0.87880900	0.60559600
H	-1.44636900	1.09768900	0.40637200
C	-2.87739600	-0.10828400	-0.16150400
H	-2.50336100	-1.67151700	-1.59028400
H	-2.90210500	0.20652900	-1.40472200
H	-1.04392200	-0.54700600	-1.22434500
O	-1.16236500	-2.39779600	0.22574700
H	-0.22302100	-2.02944900	0.27497800
H	-1.06624300	-3.24258900	-0.24457200
C	-4.25324700	-0.59045900	0.23227800
H	-4.90957300	0.26346600	0.41322200
H	-4.69478900	-1.24193900	-0.52637700
H	-4.15049600	-1.15297700	1.16566300

Table C2 Cartesian coordinates of C1Me transition state of propylene glycol in pinacol rearrangement over 3T cluster model.

Atomic Type	Coordinate (Angstroms)		
	X	Y	Z
O	1.31747100	-1.03648000	-0.13236400
Al	1.25542600	0.61167200	0.59225200
O	-0.36498000	1.26465800	0.09109800
O	1.37068500	0.36080300	2.31019000
O	2.36984900	1.67750200	-0.22870600
H	3.26219500	1.77560200	0.12396000
H	1.27556100	1.12238800	2.89485100
Si	2.51040800	-1.63710300	-1.10091500
H	2.47181000	-1.07610800	-2.48070400
H	3.88072100	-1.43872200	-0.55208800
H	2.28840800	-3.11347600	-1.22556600
Si	-0.58595000	2.68960100	-0.73491600
H	0.01159700	2.66227900	-2.09570500
H	-2.06429000	2.85686700	-0.91016200
H	-0.09105500	3.88178600	0.00284400
C	-1.90723500	-1.52277800	-0.43267400
O	-2.46188000	0.20982700	1.17570000
H	-1.60497100	0.65063600	0.83521600
C	-2.77676500	-0.85540600	0.45272800
H	-2.21827700	-2.45837300	-0.87410400
H	-1.01050400	-1.02912000	-0.78968400
O	-0.53274900	-2.67310700	0.85024300
H	0.27329300	-2.11110300	0.66687800
H	-0.29765500	-3.54921100	0.50377500
H	-3.61291800	-1.41484200	0.86871300
C	-3.42081300	-0.44914300	-1.20588100
H	-2.76195300	-0.25632800	-2.05515000
H	-4.20657300	-1.15745500	-1.46225500
H	-3.81662200	0.50678600	-0.86277200

Table C3 Cartesian coordinates of C2H transition state of propylene glycol in pinacol rearrangement over 3T cluster model.

Atomic Type	Coordinate (Angstroms)		
	X	Y	Z
O	-0.48936200	1.43925700	0.01415600
Al	-1.45137300	0.01388900	0.55131000
O	-0.48371800	-1.41118800	-0.02931600
O	-1.50502000	0.12455400	2.28717600
O	-2.92680600	-0.11331600	-0.37454900
H	-3.72796800	0.29264700	-0.02291900
H	-1.89434600	-0.60720400	2.78110100
Si	-1.03086200	2.73525200	-0.84977200
H	-1.25350500	2.41790300	-2.28864400
H	-2.28034700	3.33462500	-0.30366000
H	0.03077300	3.79083000	-0.79769400
Si	-1.06107500	-2.59724000	-1.04368800
H	-1.45772600	-2.06587400	-2.37374900
H	0.06963200	-3.55154900	-1.26791300
H	-2.18982700	-3.36749800	-0.45821100
C	2.40875400	0.00912000	-0.42686800
O	1.81300000	-1.88347700	1.01452600
H	0.85155900	-1.69880300	0.70286500
C	2.68629500	-1.15194500	0.34175900
H	3.71958800	-1.30793000	0.65950700
C	3.48814700	0.78802700	-1.11728200
H	4.48766200	0.50979400	-0.77065900
H	3.43215100	0.66443600	-2.20413100
H	3.32037600	1.84545000	-0.90499700
H	2.71029600	-1.39794300	-0.88763600
H	1.36989800	0.17047300	-0.70942600
O	1.88267200	1.47387400	1.22981300
H	0.92566300	1.56692900	0.96736900
H	2.21579800	2.38215800	1.30010600

Table C4 Cartesian coordinates of C1H transition state of propylene glycol in pinacol rearrangement over 5T cluster model.

Atomic Type	Coordinate (Angstroms)		
	X	Y	Z
O	0.64391400	1.62827800	-0.77765500
Al	0.73025100	-0.01688100	-0.10649600
O	-0.18302000	0.01678900	1.44850500
O	-0.27541400	-1.01070200	-1.17823100
O	2.33749800	-0.57519100	0.16252600
Si	1.73382200	2.84444900	-1.01375400
H	2.42968600	3.22564000	0.24858400
H	2.76932300	2.49533600	-2.02637800
H	0.99944900	4.04635000	-1.50736300
Si	0.39115800	0.10108600	3.00630500
H	1.43776300	1.14914600	3.14234000
H	-0.75236100	0.46584900	3.89266900
H	0.94329200	-1.19785300	3.47464800
C	-2.76432600	1.36561800	0.01920800
O	-2.63771700	-0.78211700	1.13094200
H	-1.66073500	-0.51779000	1.25950800
C	-3.33272700	0.14838800	0.48747900
H	-3.56395200	1.20407700	1.21206500
H	-1.82227500	1.69873600	0.43920400
O	-1.80794000	1.13492800	-1.86926900
H	-0.95721000	1.60854700	-1.69806200
H	-1.46856200	0.20571300	-1.83836600
Si	3.84995700	-1.17653500	0.09262100
H	3.90017900	-2.45807300	-0.67138300
H	4.78994700	-0.22564400	-0.57052300
H	4.38008500	-1.44965200	1.46013100
Si	-0.36178600	-2.59936300	-1.60766800
H	-1.71538700	-2.86688900	-2.17820200
H	0.64586400	-2.95775200	-2.64481500
H	-0.17008800	-3.50792800	-0.44145300
C	-4.65964200	-0.34420100	-0.03607600
H	-5.30109100	0.47540000	-0.36850300
H	-4.46000700	-1.00399800	-0.88692100
H	-5.17008800	-0.92672300	0.73427500
H	-3.40960600	2.06731600	-0.49028200

Table C5 Cartesian coordinates of C1Me transition state of propylene glycol in pinacol rearrangement over 5T cluster model.

Atomic Type	Coordinate (Angstroms)		
	X	Y	Z
O	-0.37166200	-1.33499700	-1.19952200
Al	-0.70764100	0.02110100	-0.09930800
O	0.44408800	-0.15675200	1.28204100
O	-0.16532600	1.47676200	-0.94447200
O	-2.32241000	0.04134200	0.50726100
Si	-1.18969100	-2.69541000	-1.64469300
H	-1.60362600	-3.51390700	-0.46864400
H	-2.40716400	-2.39501200	-2.44933600
H	-0.28637500	-3.53765600	-2.48356100
Si	0.14948500	-0.71578200	2.81723400
H	-0.68684900	-1.94486000	2.80506700
H	1.46810300	-1.06525000	3.42868700
H	-0.49599800	0.30673100	3.68278900
C	2.96999500	-0.60464000	-0.70469500
O	2.62428600	1.20728100	0.88503300
H	1.73528400	0.73865200	1.05866700
C	3.36577900	0.53460900	0.02031600
H	2.10989900	-1.18627700	-0.39806700
O	1.69162300	0.04990800	-2.41366100
H	0.98753100	-0.63194400	-2.32189100
H	1.19758200	0.82868300	-2.06505200
Si	-3.92446900	0.25375000	0.71573000
H	-4.33427800	1.66714500	0.46442400
H	-4.72205200	-0.61012600	-0.20397500
H	-4.32781900	-0.08679000	2.11117900
Si	-0.50895200	3.08733200	-0.92676500
H	0.59242600	3.82249200	-1.61389500
H	-1.77927000	3.39981000	-1.64073400
H	-0.61884900	3.62364600	0.46082600
H	3.60198000	-0.96162600	-1.50291000
H	4.20639600	1.11248500	-0.35859400
C	4.15906100	-0.91108800	0.86647500
H	4.69782500	-1.70996200	0.35682500
H	3.43848000	-1.27877200	1.59385600
H	4.88306700	-0.25188200	1.34824100

Table C6 Cartesian coordinates of C2H transition state of propylene glycol in pinacol rearrangement over 5T cluster model.

Atomic Type	Coordinate (Angstroms)		
	X	Y	Z
O	0.11597100	1.58733300	-0.69025400
Al	0.70460500	0.01523500	-0.10615500
O	-0.22336700	-0.33228400	1.40686100
O	0.13186900	-1.18967500	-1.26494600
O	2.39219900	-0.00471700	0.24878900
Si	0.77619000	3.08526000	-0.88113100
H	1.35700500	3.61012800	0.38816400
H	1.84123300	3.11472000	-1.92281500
H	-0.30132900	4.02780800	-1.30588800
Si	0.28266400	-0.20156900	2.98582900
H	0.97627700	1.09079300	3.22839300
H	-0.93442500	-0.24546400	3.84973600
H	1.17529600	-1.31947600	3.39028900
C	-3.18409200	0.41341500	0.23001000
O	-2.33585800	-1.74648900	1.01309300
H	-1.44831700	-1.24368500	1.13944800
C	-3.30388500	-0.94772800	0.60921500
H	-4.21952700	-1.47334200	0.33013200
C	-4.35129900	1.19404100	-0.29925100
H	-5.26467100	0.59201600	-0.33050700
H	-4.52998500	2.09641900	0.29277200
H	-4.09955300	1.49179500	-1.31970400
H	-3.70890700	-0.10962300	1.48879000
H	-2.27829700	0.92696900	0.53844200
O	-2.09219600	0.37425900	-1.80694900
H	-1.40308100	1.05835200	-1.63877200
H	-1.51674900	-0.42365500	-1.84020700
Si	4.01973100	-0.06792200	0.22444100
H	4.51729400	-1.25808500	-0.52675100
H	4.61003400	1.14265000	-0.41933100
H	4.57009200	-0.15100100	1.60882400
Si	0.65156100	-2.62346400	-1.88466800
H	-0.46389300	-3.24817800	-2.65381000
H	1.80452300	-2.45247400	-2.81388000
H	1.06179800	-3.58279400	-0.81849400

Table C7 Cartesian coordinates of transition state of pinacol rearrangement over 3T cluster model.

Atomic Type	Coordinate (Angstroms)		
	X	Y	Z
O	1.61002700	-1.30722300	-0.23685600
Al	1.77756900	0.20966500	0.70389200
O	0.75757800	1.45268200	-0.11736300
O	1.07974000	-0.18747800	2.28072700
O	3.39115200	0.86656700	0.66256500
H	4.09747000	0.37363700	1.09721500
H	1.15670000	0.48612200	2.96828700
Si	2.78466900	-2.17669600	-0.99194700
H	3.35218100	-1.47658800	-2.18102700
H	3.92426900	-2.52383700	-0.09106000
H	2.19700900	-3.46218000	-1.47731300
Si	1.25532400	2.86191900	-0.83432200
H	2.32596600	2.64307400	-1.84230100
H	0.07292800	3.43243400	-1.55276300
H	1.71348200	3.88156800	0.14840300
C	-2.30923000	-0.62962300	-0.67115200
O	-1.75495700	1.40992800	0.52652600
H	-0.79246300	1.32839800	0.20445200
C	-2.57226900	0.36210000	0.31963700
C	-3.02984600	-1.94147300	-0.69038000
H	-3.96434000	-1.94487800	-0.12977600
H	-3.20957500	-2.28237300	-1.71387600
H	-2.34891300	-2.64293900	-0.19120500
O	-0.70402100	-1.95866300	1.25169000
H	0.07228900	-2.10710800	0.67472700
H	-0.27797700	-1.39215900	1.93561100
C	-3.39201400	0.05318800	1.56053900
H	-3.64433000	0.99767800	2.04769100
H	-4.30888400	-0.50587400	1.36484900
H	-2.75862300	-0.53393500	2.23142400
C	-1.23322300	-0.44515600	-1.68852500
H	-0.32214900	-0.92256500	-1.29357000
H	-1.49720600	-0.93040100	-2.63261400
H	-0.97464400	0.59981100	-1.85700400
C	-3.73381100	0.83629400	-0.96492400
H	-4.57678700	0.16662600	-1.12581900
H	-3.27064900	1.16087400	-1.89473000
H	-4.04784300	1.71738100	-0.40190700

Table C8 Cartesian coordinates of transition state of pinacol rearrangement over 5T cluster model.
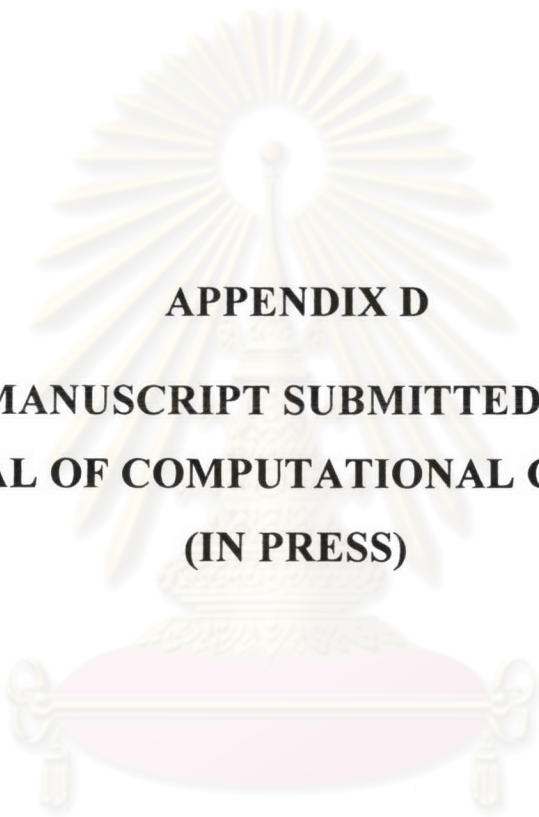
Atomic Type	Coordinate (Angstroms)		
	X	Y	Z
O	0.78804200	1.72262000	-0.53874900
Al	1.28679900	0.06206100	-0.12955600
O	0.31752100	-0.42171400	1.30985500
O	0.78181500	-0.97063600	-1.46953800
O	2.96417500	-0.02591200	0.28870800
Si	1.60373400	3.15263100	-0.61361500
H	2.17815900	3.55023700	0.70416300
H	2.70905500	3.13723000	-1.61301100
H	0.64187800	4.22131300	-1.02046700
Si	0.86250200	-0.85567500	2.81457200
H	1.74258600	0.18309800	3.41399300
H	-0.33403200	-1.00258500	3.69781000
H	1.58732300	-2.15512000	2.81071400
C	-3.06696600	0.75013400	0.19531800
O	-2.04196400	-1.37545900	0.75413500
H	-1.17104900	-0.89060300	0.94401200
C	-3.01956400	-0.67457100	0.14790700
C	-3.96442200	1.54716800	-0.69862900
H	-4.71853000	0.95261700	-1.21281200
H	-4.44235800	2.36486300	-0.15049600
H	-3.30792000	1.97312200	-1.46682600
O	-1.36637100	0.77453000	-2.03824900
H	-0.69200900	1.40013100	-1.70142800
H	-0.79963600	-0.01623400	-2.14740300
C	-3.63552000	-1.46677400	-0.99309000
H	-3.64230500	-2.52128100	-0.70925000
H	-4.64878300	-1.15954700	-1.25751200
H	-2.99014500	-1.34303800	-1.86698100
C	-2.17749900	1.52740800	1.11165200
H	-1.26138100	1.79247400	0.56269800
H	-2.66417800	2.45226400	1.43453200
H	-1.84957300	0.95010900	1.97621900
C	-4.32960100	-0.41174500	1.34644100
H	-5.28087800	-0.11578200	0.90900500
H	-4.07443500	0.17510700	2.22753200
H	-4.33614400	-1.46804600	1.62214100
Si	0.96858800	-2.52248200	-1.96816500
H	1.35523000	-3.44077200	-0.85704700
H	-0.32122200	-3.02410500	-2.53445900
H	1.99657300	-2.64589800	-3.04084200
Si	4.55894300	-0.35011900	0.27036000
H	5.36355800	0.87229400	-0.02518200

Table C9 Cartesian coordinates of transition state of pinacol rearrangement over Fe-3T cluster model.

Atomic Type	Coordinate (Angstroms)		
	X	Y	Z
O	0.81168800	1.36524300	-0.31845500
Al	1.97497500	0.65064700	0.90296500
O	1.84043900	-0.95952500	0.01873400
O	3.43121700	1.54084700	0.78158700
O	1.14983300	0.32889000	2.40684600
H	1.35588900	0.85073400	3.19291500
H	4.17323400	1.51043800	1.39459000
Si	0.90766500	2.90357600	-1.00415400
H	-0.40346600	3.15803700	-1.66024100
H	1.13459800	3.91193400	0.05658400
H	1.97616000	2.95080200	-2.02969200
Si	2.43614600	-2.45891000	0.49490300
H	1.32405800	-3.28202800	1.03831800
H	2.99451400	-3.13765000	-0.70309300
H	3.48952300	-2.26887600	1.51878100
Fe	0.19999900	-0.43513800	-1.01134000
O	0.51480000	-1.71398000	-2.63352100
O	-1.67463000	-0.56343100	-1.00054000
C	-2.62243900	-0.14063600	1.16895000
C	-2.66015500	-0.00363300	-0.27176300
H	1.35653700	-1.90557700	-3.07907300
C	-3.22408100	1.26684800	-0.91554000
H	-4.14619500	1.63429900	-0.46196600
H	-2.46678300	2.05509200	-0.86520700
H	-3.41702800	1.05326300	-1.96949600
C	-1.67893100	-1.08589600	1.80644700
H	-0.79015700	-0.49726900	2.12900200
H	-2.09616000	-1.54168400	2.70936900
H	-1.31833400	-1.85060600	1.11781700
C	-3.47950700	0.66700600	2.08375000
H	-2.79796200	1.34089100	2.62600600
H	-4.22771800	1.27983500	1.58398500
H	-3.95529000	0.03802300	2.84372900
H	-0.20736700	-1.96823200	-3.23115400
C	-3.94641100	-1.13476400	-0.17576900
H	-4.86897600	-0.74146900	0.24888000
H	-4.04959000	-1.26807900	-1.25577000
H	-3.66511000	-2.08990600	0.26786800

Table C10 Cartesian coordinates of transition state of pinacol rearrangement over Cu-3T cluster model.

Atomic Type	Coordinate (Angstroms)		
	X	Y	Z
O	0.62980900	1.28520600	-0.40026200
Al	1.94207200	0.85788100	0.82334000
O	1.88850400	-0.83427200	0.10630800
O	3.27794400	1.84752800	0.41638500
O	1.28370800	0.69813200	2.42047500
H	1.53322400	1.31501600	3.11988200
H	4.03343600	2.05458300	0.97637500
Si	0.62374500	2.70151300	-1.32383100
H	-0.69898100	2.77784500	-1.99510200
H	0.78886500	3.86264800	-0.42156500
H	1.67911200	2.65510700	-2.36103400
Si	2.61540500	-2.27768400	0.57915400
H	1.60711300	-3.14755500	1.23590000
H	3.13289300	-2.96158200	-0.63347800
H	3.72254600	-1.96113100	1.50984800
O	0.46060700	-2.11164100	-2.08636000
O	-1.61650800	-0.81466800	-0.91038800
C	-2.57334300	0.01947700	1.12894500
C	-2.55950300	-0.09775700	-0.30499000
H	1.23154000	-2.26195400	-2.65751200
C	-3.25574900	0.90054800	-1.21644600
H	-4.03193000	1.49887000	-0.73796300
H	-2.49105900	1.57565400	-1.60912200
H	-3.69395800	0.36826400	-2.06510200
C	-1.61656200	-0.77162900	1.96696600
H	-0.79490300	-0.10545600	2.28732900
H	-2.10343000	-1.13888700	2.87538100
H	-1.17593800	-1.60744600	1.42340000
C	-3.43842900	0.98583400	1.88458200
H	-2.77346400	1.74582100	2.31857300
H	-4.18223400	1.50041700	1.27739100
H	-3.93328800	0.48877700	2.72511500
H	-0.33169600	-2.45527900	-2.53131500
C	-3.87471000	-1.25226600	0.25388800
H	-4.81006900	-0.74997500	0.49045400
H	-3.89180800	-1.68681300	-0.74631100
H	-3.61754400	-2.02811500	0.97304600
Cu	0.23185500	-0.55491000	-0.84065700

APPENDIX D

**MANUSCRIPT SUBMITTED TO
JOURNAL OF COMPUTATIONAL CHEMISTY
(IN PRESS)**

A Density Functional Study of Propylene Glycol Conversion to Propanal and Propanone of Various Acid-Catalyzed Reaction Models: A Water-Addition Effect

CHOMPOONUT RUNGNIM, VITHAYA RUANGPORNVISUTI

Supramolecular Chemistry Research Unit, Department of Chemistry, Faculty of Science, Chulalongkorn University 10330, Bangkok, Thailand

Correspondence to: V. Ruangpornvisuti; e-mail: vithaya.r@chula.ac.th

ABSTRACT: The acid-catalyzed models on reaction mechanisms of pinacol rearrangement of propylene glycol conversion to propanal and propanone have been investigated using density functional method at 298.15 K. Thermodynamic quantities of activation steps of four water-addition models were obtained. The number of added water interacting with the transition states of three concerted pathways has obviously affected the product ratio. The relative energetic profiles of the conversion reactions of all solvation models have been comparatively displayed. Estimation of percent ratio of product composition computed from activation free energies of each acid-catalyzed reaction models were carried out. The percent ratios of propanal and propanone were decreased as the number of added water increased.

Key words: density functional theory; acid-catalyzed models; propylene glycol; propanal; propanone; rate constant

Introduction

The pinacol rearrangement in the conversion of glycol to propanal was reviewed by Wheland.[1] The pinacol rearrangement has been described to proceed only with a stepwise mechanism via carbocation intermediate which was first introduced by Whitmore.[2] The reaction mechanism and migratory aptitude of the pinacol rearrangement were theoretically examined for protonated 1,2-ethanediols using RHF/6-31G method.[3] The rearrangements of many reactions were found where they have involved not only the stepwise but also the concerted mechanism.[3-6] Smith and

RHF/6-31G method.[3] The rearrangements of many reactions were found where they have involved not only the stepwise but also the concerted mechanism.[3-6] Smith and coworker[7] applied the E2 process of dehydration mechanism in the elimination reactions of 2-bromobutane in water. Two possible mechanisms of ethylene glycol conversion to acetaldehyde were proposed by Smith[8] using the theoretical approaches. The dehydration mechanism were energetically compared to the pinacol rearrangement of concerted mechanism and the latter process was shown proceed at a lower activation enthalpy than the dehydration mechanism by 69.8 kcal mol^{-1}.[8] Recently, the dehydration of ethylene glycol in near-critical water with the zinc chloride catalyst   to obtain hydrolysis product 2-methyl-2-pentenal has been carried out.[9] Nevertheless, several reports supported that the pinacol rearrangement does not proceed by the stepwise mechanism[10,11] and in the gas phase the stepwise mechanism being less favored than the concerted mechanism has been found. [12-14] In present work, the pinacol rearrangement of propylene glycol conversion to propanal and propanone at various acid-catalyzed models has been therefore theoretically investigated via the concerted mechanism by density functional method. The concerted mechanism of the system respectively including one-, two- and three-waters clusters defined as models II, III and IV have been investigated in order to observe their reaction products. The product composition of various acid-catalyzed models has been evaluated in order to get more understanding of the effect of the added water on the reaction products.

Computational method

Full geometry optimizations of entities were computed by density functional theory (DFT).   Density functional calculations have been performed with the Becke's three parameters hybrid density functional using the Lee, Yang and Parr correlation functional (B3LYP).[15,16] All geometry optimizations have been carried out using the hybrid density functional B3LYP with the 6-31G(d) basis set. The energies of the B3LYP/6-31G(d) optimized geometries have been calculated with the zero-point energy corrections. The B3LYP/6-31G(d,p) and B3LYP/6-311G(d,p) levels of theory were employed for the single point calculations of the B3LYP/6-31G(d) optimized geometries of involved species. The transition states have been located using the

frequency. The intrinsic reaction coordinate (IRC) method [18] was used to track minimum energy paths from transition structures to the corresponding minimum. All calculations were performed with the Gaussian 03 program.[19] The MOLDEN 4.2 program[20] was utilized to display molecular structures and observe the geometry convergence via the Gaussian output files. The molecular graphics of all species were generated with the MOLEKEL 4.3 program.[21]

The standard enthalpy ΔH^O and Gibbs free energy changes ΔG^O of conversion reactions of this system have been derived from the frequency calculations at B3LYP/6-31G(d) level of theory. The rate constant $k(T)$ derived from transition state theory was computed from activation free energy, $\Delta^{\ddagger}G^O$ by using $k(T) = \dfrac{k_B T}{h c^o} \exp(-\Delta^{\ddagger}G^O/RT)$ where concentration factor, c^o of unity is used, k_B is Boltzmann's constant, h is Plank's constant, T is the absolute temperature and R is gas constant.[22] The above formula was employed to compute the reaction rate constants for corresponding activation free energies as introduced in previous works.[23-24]

The multi-transition-state system introduced by Adam [25] was extended for the Curtin-Hammett principle [26] which is the two competitive transition states. As the present work is a tri-transition-state system without pre-reaction cluster, the reaction scheme of this system is therefore reduced as shown in Figure 1. According to transition state theory, the rate constant for each individual reaction i is given by equation 1. [27]

$$k_i(T) = \frac{k_B T}{h c^o} \exp(-\Delta^{\ddagger}G_i^O/RT) \tag{1}$$

Where $\Delta^{\ddagger}G_i^O = G_i^{TS,O} - G_o^O$, i is the rank of reaction paths (i = 1, 2 and 3) and $G_i^{TS,O}$ and G_o^O are Gibbs free energies of transition state and corresponding reactant, respectively. As transition states TS1 and TS2 step forward to protonated form of propanal product (HPPNL$^+$) and TS3 to protonated form of propanone product (HPPNE$^+$), the product ratio of [HPPNL$^+$] to [HPPNE$^+$] is therefore equivalent to the ratio of the sums of all ground-state population of reactants P_o and its corresponding rate constants forward to product [HPPNL$^+$] to sums for [HPPNE$^+$]. Therefore, the [HPPNL$^+$] to [HPPNE$^+$] ratio can be given by equation 2.
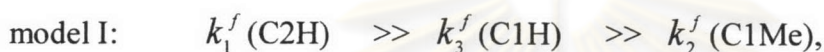
$$\frac{[\text{HPPNL}^+]}{[\text{HDPNE}^+]} = \frac{P_o k_1 + P_o k_2}{P_o k_3} = \frac{k_1 + k_2}{k_3}$$

$$= \frac{\sum_{i=1}^{2} \exp(-\Delta^{\ddagger} G_i^O / RT)}{\exp(-\Delta^{\ddagger} G_3^O / RT)} = \frac{\exp(-\Delta^{\ddagger} G_1^O / RT) + \exp(-\Delta^{\ddagger} G_2^O / RT)}{\exp(-\Delta^{\ddagger} G_3^O / RT)} \qquad (2)$$

Where k_1, k_2 and k_3 are forward rate constants of reaction pathways 1, 2 and 3, respectively as shown in Figure 1. In present work, four acid-catalyzed models with respect to the increased numbers of added water were investigated for the effect of added water to product compositions. Model I is an acid-catalyzed model of a gas-phase system which is composed of one proton as acid catalytic atom without solvation water except a dehydration water which is released from the reaction. Model II is an acid-catalyzed model of which the reactant is protonated by a single proton of which the molecule is hydrated by one water molecule. Models III and IV are acid-catalyzed models of which protonated species are hydrated by one and two water molecules, respectively.

Results and discussion

All structures were optimized using DFT at B3LYP/6-31G(d) level of theory. The zero point energies and thermodynamic quantities of activation steps were derived from the frequency calculations at 298.15 K at the same level of theory. Reaction mechanisms of propylene glycol (PG) conversion to propanal (PPNL) and propanone (PPNE) of various acid-catalyzed water-addition models of three concerted pathways were found. This conversion reaction has been investigated using the protonated forms of propylene glycol (HPG$^+$), propanal (HPPNL$^+$) and propanone (HPPNE$^+$). A representative scheme of a concerted reaction mechanism of propylene glycol conversion to propanal and propanone via transition states TS1, TS2 and TS3 which are the secondary and primary carbonium ions is shown in Figure 2. Total energies and geometrical structures of species HPG$^+$, HPPNL$^+$ and HPPNE$^+$ and the corresponding transition states of various acid-catalyzed models were determined at the B3LYP/6-31G(d) level of theory with zero point energy corrections. The

corresponding transition states of various acid-catalyzed models were determined at the B3LYP/6-31G(d)   level of theory with zero point energy corrections. The activation thermodynamic quantities, forward and backward rate constants of acid-catalyzed reaction models I, II, III and IV are shown in Table 1, 2, 3 and 4, respectively.   The three concerted pathways (1) C1H, (2) C1Me and (3) C2H via transition states TS1 and TS2, and TS3 have afforded the products HPPNL$^+$ and HPPNE$^+$, respectively. Figure 1 shows that the product HPPNL$^+$ was produced via transition states TS1 and TS2 and HPPNE$^+$ via transition state TS3. The magnitude orders of forward rate constants of four reaction models as tabulated in Table 1, 2, 3 and 4 are concluded as

model I: k_1^f (C2H) $\gg$ k_3^f (C1H) $\gg$ k_2^f (C1Me),

model II: k_1^f (C2H) $\gg$ k_3^f (C1H) $\gg$ k_2^f (C1Me),

model III: k_1^f (C2H) $>$ k_3^f (C1H) $\gg$ k_2^f (C1Me),

model IV: k_3^f (C1H) $\sim$ k_1^f (C2H) $\gg$ k_2^f (C1Me).

The typical structures of transition states TS1, TS2 and TS 3 are the secondary (C2H), primary (C1Me) and primary (C1H) carbonium cations, respectively. As the decreasing order of structural stability of carbonium ions is as tertiary > secondary > primary, the secondary carbonium ion of transition state TS1 (C2H) is the stable species in gas-phase which is much more stable than the transition states TS2 and TS3 in gas-phase which is defined as model I. As the primary carbonium ions of transition states TS2(C1Me) and TS3(C1H) are stabilized in aqueous-phase which is defined as model IV, the tri-solvation of TS3(C1H) was found to be more stable than its mono-solvation in model I. The stability order of transition state TS3 with respect to TS1 and TS2 is remarkably changed at high number of solvation water of model IV as shown in following scheme,

Relative stability

TS2 → TS2 → TS2 → TS2

TS3 → TS3 → TS3 → TS1
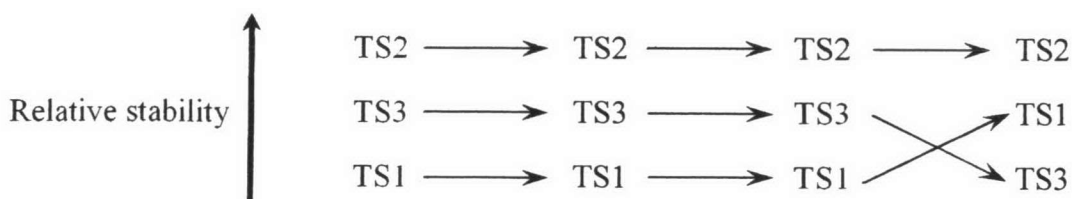
TS1 → TS1 → TS1 → TS3

B3LYP/6-31G(d)//B3LYP/6-31G(d),   B3LYP/6-31G(d,p)//B3LYP/6-31G(d)   and B3LYP/6-311G(d)//B3LYP/6-31G(d) levels of theory are tabulated in Table 5. Table 5 shows that the activation energies derived from the total energies of transition states TS1, TS2 and TS3 using single point calculations are in the same order of magnitudes with respect to the B3LYP/6-31G(d) energies of zero-point energy corrections. The reactant HPG$^+$, transition states TS1, TS2 and TS3 and products HPPNL$^+$ and HPPNE$^+$ in model I, II, III, IV and V are shown in Figures 4, 5, 6 and 7, respectively. The O…H distance of hydrogen bond of intermolecular interaction between water molecule(s) and involved species and their dipole moments are shown in Figures 4, 5, 6 and 7. The percent compositions of products HPPNL$^+$ and HPPNE$^+$ derived from equation 2 are tabulated in Table 6. The models I, II and III in Table 6 result that the HPPNL$^+$ is the dominant product of which percent are larger than 85 %. For the product ratio of HPPNL$^+$ to HPPNE$^+$ of the model IV is 46.59 to 53.41. However, the experimental values of the ratio HPPNL$^+$ to HPPNE$^+$ in acidic aqueous solution have been not found but the amino alcohol $CH_3CC_6H_5C(OH)CH_2NH_2$ conversion reaction, the distribution ratio (in %) of products $C_6H_5CH_2CHOCH_3$ (benzyl methyl ketone) is 75 to 25.[28]

Conclusions

The zero point energies and thermodynamic quantities of activation steps were obtained at B3LYP/6-31G(d) level of theory. Reaction mechanisms of propylene glycol (PG) conversion to propanal (PPNL) and propanone (PPNE) of various acid-catalyzed water-addition models of three concerted pathways were investigated using the protonated forms of propylene glycol (HPG$^+$), propanal (HPPNL$^+$) and propanone (HPPNE$^+$). The three concerted pathways C2H, C1Me and C1H via transition states TS1 and TS2, and TS3 have produced the products HPPNL$^+$ and HPPNE$^+$, respectively.   The percent ratios of product HPPNL$^+$ to HPPNE$^+$ based on models I, II III and IV are [99.88]:[0.12], [99.81]:[0.19], [89.01]:[10.99] and [46.59]:[53.41], respectively.

References

1. Wheland, G. W. Advanced Organic Chemistry; Wiley: New York, 1949 p 23.

2. Whitmore, F. C. J Am Chem Soc 1932, 54, 3274.

3. Barili, P. L.; Berti, G.; Macchia, B.; Macchia, F.; Monti, L. J Chem Soc C 1970, 1168.

4. Berti, G.; Macchia, B.; Macchia, F.; Monti, L. J Chem Soc C 1971, 3371.

5. Stiles, M.; Mayer, R.P. J Am Chem Soc 1959, 81, 1497.

6. Nakamura, K.; Osamura, Y. J. Am Chem Soc 1993, 115, 9112.

7. Smith, W. B.; Watson, W. H. J Am Chem Soc 1962, 84, 3174.

8. Smith, W. B. Tetrahedron 2002, 58, 2091.

9. Dai, Z.; Hatano, B.; Tagaya, H. Appl Cat 2004, 258, 189.

10. Stiles, M.; Mayer, R. P. Am Chem Soc 1959, 81, 1497.

11. Nakamura, K.; Osamura, Y. J. Phys Org chem. 1990, 3, 737.

12. Petris, G. de.; Giacomello, P.; Picotti, T.; Pizzabiocca, A.; Renzi, G.; Speranza, M. Am Chem Soc 1986, 108, 7491.

13. Petris, G. de.; Giacomello, P.; Pizzabiocca, A.; Renzi, G.; Speranza, M. Am Chem Soc 1988, 110, 1098.

14. Toda, F.; Shigemasa, T. J Chem Soc Perkin Trans 1 1989, 209.

15. Becke, A. D. Phys Rev 1988, A38, 3098.

16. Lee, C.; Yang, W.; Parr, R.G. Phys Rev 1988, B37, 385.

17. Peng, C.; Ayala, P. Y.; Schlegel, H. B.; Frisch, M. J. J Comp Chem 1996, 17, 49.

18. Gonzales, C.; Schlegel, H.B. J Chem Phys 1989, 90, 2154.

19. Frisch, M. J.; Trucks, G. W.; Schlegel, H. B.; Scuseria, G. E.; Robb, M. A.; Cheeseman, J. R.; Montgomery, Jr., J. A.; Vreven, T.; Kudin, K. N.; Burant, J. C.; Millam, J. M.; Iyengar, S. S.; Tomasi, J.; Barone, V.; Mennucci, B.; Cossi, M.; Scalmani, G.; Rega, N.; Petersson, G. A.; Nakatsuji, H.; Hada, M.; Ehara, M.; Toyota, K.; Fukuda, R.; Hasegawa, J.; Ishida, M.; Nakajima, T.; Honda, Y.; Kitao, O.; Nakai, H.; Klene, M.; Li, X.; Knox, J. E.; Hratchian, H. P.; Cross, J. B.; Adamo, C.; Jaramillo, J.; Gomperts, R.; Stratmann, R. E.; Yazyev, O.; Austin, A. J.; Cammi, R.; Pomelli, C.; Ochterski, J. W.; Ayala, P. Y.; Morokuma, K.; Voth, G. A.; Salvador, P.; Dannenberg, J. J.; Zakrzewski, V. G.; Dapprich, S.; Daniels, A. D.; Strain, M. C.; Farkas, O.; Malick, D. K.; Rabuck, A. D.;

Raghavachari, K.; Foresman, J. B.; Ortiz, J. V.; Cui, Q.; Baboul, A. G.; Clifford, S.; Cioslowski, J.; Stefanov, B. B.; Liu, G.; Liashenko, A.; Piskorz, P.; Komaromi, I.; Martin, R. L.; Fox, D. J.; Keith, T.; Al-Laham, M. A.; Peng, C. Y.; Nanayakkara, A.; Challacombe, M.; Gill, P. M. W.; Johnson, B.; Chen, W.; Wong, M. W.; Gonzalez, C.; and Pople, J. A.; Gaussian 03, Gaussian, Inc., Pittsburgh PA, 2003.

20. Molden 4.2 : Schaftenaar, G., CAOS/CAMM Center Nijmegen, Toernooiveld, Nijmegen, Netherlands, 1991.

21. Flükiger, P.; Lüthi, H. P.; Portmann, S.; Weber, J., Molekel 4.3: Swiss Center for Scientific Computing, Manno (Switzerland), 2000.

22. Ochterski, J.W., Thermochemistry in Gaussian, Gaussian Inc., 2000.

23. Thipyapong, K.; Arano, Y.; Ruangpornvisuti, V. J Mol Struct (Theochem) 2004, 676, 65.

24. Ruangpornvisuti, V.; Wanno B. J Mol Model 2004, 10, 418.

25. Adam, W.; Bach, R.D.; Dmitrenko, O.; Saha-Möller, C.R. J Org Chem 2000, 65, 6715.

26. Curtin, D.Y. Rec Chem Prog 1954, 15, 111.

27. Eyring, H. J Chem Phys 1935, 3, 107.

28. House, H.O.; Grubbs, E. J. J Am Chem 1959, 81, 4733.

Table 1. Activation Thermodynamic Quantities and Rate Constants of Acid-Catalyzed Reaction Model I.

Reactions			$\Delta^{\ddagger}H^{O}$ [a]	$\Delta^{\ddagger}G^{O}$ [a]	k [b]
C2H pathway					
k_1^f : HPG$^+$	$\longrightarrow$	TS1	20.19	16.37	6.21×10^{0}
k_1^b : HPPNL$^+$	$\longrightarrow$	TS1	36.45	35.87	3.16×10^{-14}
C1Me pathway					
k_2^f : HPG$^+$	$\longrightarrow$	TS2	25.90	23.17	6.40×10^{-5}
k_2^b : HPPNL$^+$	$\longrightarrow$	TS2	42.17	42.67	3.26×10^{-19}
C1H pathway					
k_3^f : HPG$^+$	$\longrightarrow$	TS3	22.25	20.36	7.32×10^{-3}
k_3^b : HPPNE$^+$	$\longrightarrow$	TS3	52.56	54.09	1.39×10^{-27}

[a] in kcal mol^{-1}. [b] forward (k^f) and backward (k^b) rate constants, in s^{-1}.

Table 2. Activation Thermodynamic Quantities and Rate Constants of Acid-Catalyzed Reaction Model II.

Reactions			$\Delta^{\ddagger}H^{O}$ [a]	$\Delta^{\ddagger}G^{O}$ [a]	k [b]
C2H pathway					
k_1^f : HPG$^+$	$\longrightarrow$	TS1	27.58	24.26	1.01×10^{-5}
k_1^b : HPPNL$^+$	$\longrightarrow$	TS1	37.40	37.85	1.12×10^{-15}
C1Me pathway					
k_2^f : HPG$^+$	$\longrightarrow$	TS2	33.77	30.12	5.20×10^{-10}
k_2^b : HPPNL$^+$	$\longrightarrow$	TS2	43.60	43.70	5.76×10^{-20}
C1H pathway					
k_3^f : HPG$^+$	$\longrightarrow$	TS3	29.97	27.97	1.96×10^{-8}
k_3^b : HPPNE$^+$	$\longrightarrow$	TS3	53.58	55.64	1.01×10^{-28}

[a] in kcal mol^{-1}. [b] forward (k^f) and backward (k^b) rate constants, in s^{-1}.

Table 3. Activation Thermodynamic Quantities and Rate Constants of Acid-Catalyzed Reaction Model III.

Reactions		$\Delta^{\ddagger}H^{O}$ [a]	$\Delta^{\ddagger}G^{O}$ [a]	k [b]
C2H pathway				
k_1^f : HPG$^+$ $\longrightarrow$	TS1	29.91	26.79	1.42×10^{-7}
k_1^b : HPPNL$^+$ $\longrightarrow$	TS1	46.21	46.93	2.45×10^{-22}
C1Me pathway				
k_2^f : HPG$^+$ $\longrightarrow$	TS2	36.17	32.38	1.14×10^{-11}
k_2^b : HPPNL$^+$ $\longrightarrow$	TS2	52.46	52.52	1.97×10^{-26}
C1H pathway				
k_3^f : HPG$^+$ $\longrightarrow$	TS3	29.94	28.03	1.75×10^{-8}
k_3^b : HPPNE$^+$ $\longrightarrow$	TS3	55.20	56.58	2.08×10^{-29}

[a] in kcal mol^{-1}. [b] forward (k^f) and backward (k^b) rate constants, in s^{-1}.

Table 4. Activation Thermodynamic Quantities and Rate Constants of Acid-Catalyzed Reaction Model IV.

Reactions		$\Delta^{\ddagger}H^{O}$ [a]	$\Delta^{\ddagger}G^{O}$ [a]	k [b]
C2H pathway				
k_1^f : HPG$^+$ $\longrightarrow$	TS1	26.45	21.07	2.23×10^{-3}
k_1^b : HPPNL$^+$ $\longrightarrow$	TS1	48.09	49.06	6.71×10^{-24}
C1Me pathway				
k_2^f : HPG$^+$ $\longrightarrow$	TS2	32.37	27.25	6.51×10^{8}
k_2^b : HPPNL$^+$ $\longrightarrow$	TS2	54.01	55.25	1.96×10^{-28}
C1H pathway				
k_3^f : HPG$^+$ $\longrightarrow$	TS3	25.27	20.99	2.56×10^{-3}
k_3^b : HPPNE$^+$ $\longrightarrow$	TS3	56.87	59.47	1.58×10^{-31}

[a] in kcal mol^{-1}. [b] forward (k^f) and backward (k^b) rate constants, in s^{-1}.

Table 5. Activation Energies of the Conversion Reaction of Various Acid-Catalyzed Models Computed at Various DFT Methods.

Transition structures	ΔE_{rel}^{O} [a]				
	B3LYP/6-31G(d)// B3LYP/6-31G(d) [b]	B3LYP/6-31G(d)// B3LYP/6-31G(d) [c]	B3LYP/6-31G(d)// B3LYP/6-31G(d)	B3LYP/6-31G(d,p)// B3LYP/6-31G(d)	B3LYP/6-311G(d,p)// B3LYP/6-31G(d)
Model I					
TS1	18.65	18.28	24.20	23.14	19.76
TS2	24.73	24.25	28.53	28.20	25.68
TS3	21.44	21.02	25.78	24.90	22.51
Model II					
TS1	26.25	25.73	30.84	30.20	26.93
TS2	32.51	31.88	36.21	36.32	33.67
TS3	29.13	28.56	33.32	32.86	30.36
Model III					
TS1	28.80	28.23	33.23	32.54	28.99
TS2	34.89	34.21	38.38	38.48	35.31
TS3	29.28	28.71	33.11	32.59	29.76
Model IV					
TS1	24.45	23.97	27.32	26.29	21.94
TS2	30.51	29.91	31.74	31.59	27.85
TS3	24.71	23.24	27.32	25.12	21.59

[a] in kcal mol^{-1}. [b] with ZPE corrections. [c] with ZPE corrections, scaled by 0.9804.[22]

Table 6. Percent of Product Compositions of HPPNL$^+$ and HPPNE$^+$ and Its Ratio based upon the B3LYP/6-31G(d) Computation.

Model	[HPPNL$^+$] [a]	[HPPNE$^+$] [a]	[HPPNL$^+$]:[HPPNE$^+$] [b]
I.	99.88	0.12	848.13
II.	99.81	0.19	516.65
III.	89.01	10.99	8.10
IV.	46.59	53.41	0.87

[a] in percent. [b] Computed using equation 2.

Captions for the illustrations

Figure 1. Tri-transition-state reaction for the formation of the two products of HPPNL$^+$ and HPPNE$^+$.

Figure 2. A representative scheme of reaction mechanism and the secondary and primary carbonium ions of transition states TS1(C2H) and TS2(C1Me) and TS3(C1H), respectively.

Figure 3. Relative energetic profiles of conversion reactions of (a) model I, (b) model II, (c) model III and (d) model IV. All energies (in kcal mol^{-1}) are based upon total energies with respect to reactant HPG$^+$ computed at B3LYP/6-31G(d) level of theory with zero-point energy corrections.

Figure 4. The B3LYP/6-31G(d) optimized geometries of conversion reaction model I of transition states, reactants and two products. Hydrogen bond distances are in angstroms. The imaginary frequencies of transition states are in parentheses.

Figure 5. The B3LYP/6-31G(d) optimized geometries of conversion reaction model II of transition states, reactants and two products.

Figure 6. The B3LYP/6-31G(d) optimized geometries of conversion reaction model III of transition states, reactants and two products.

Figure 7. The B3LYP/6-31G(d) optimized geometries of conversion reaction model IV of transition states, reactants and two products.
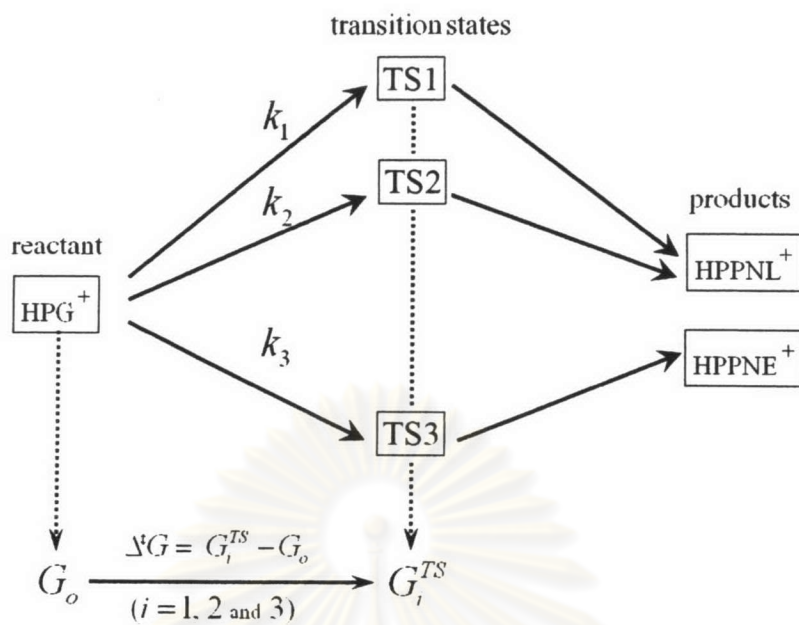
Figure 1.

Figure 2.

Figure 3.

TS1
(603i cm⁻¹), μ=2.089 D

TS2
(401i cm⁻¹), μ=1.341 D

TS3
(657i cm⁻¹), μ=2.053 D

HPG⁺
μ=1.290 D

HPPNL⁺
μ=2.441 D

HPPNE⁺
μ=1.774 D

Figure 4.

TS1
(571i cm⁻¹), µ=1.130 D

TS2
(416i cm⁻¹), µ=0.728 D

TS3
(628i cm⁻¹), µ=2.064 D

HPG⁺
µ= 3.877 D

HPPNL⁺
µ=4.212 D

HPPNE⁺
µ=2.159 D

Figure 5.

TS1
(725i cm⁻¹), µ=1.935 D

TS2
(483i cm⁻¹), µ=1.121 D

TS3
(762i cm⁻¹), µ=1.616 D

HPG⁺
µ=3.155 D

HPPNL⁺
µ=5.563 D

HPPNE⁺
µ=4.228 D

Figure 6.

TS1
(756i cm⁻¹), μ=1.604 D

TS2
(512i cm⁻¹), μ=0.609 D

TS3
(832i cm⁻¹), μ=0.976 D

HPG⁺
μ= 2.304 D

HPPNL⁺
μ=6.876 D

HPPNE⁺
μ=6.607 D
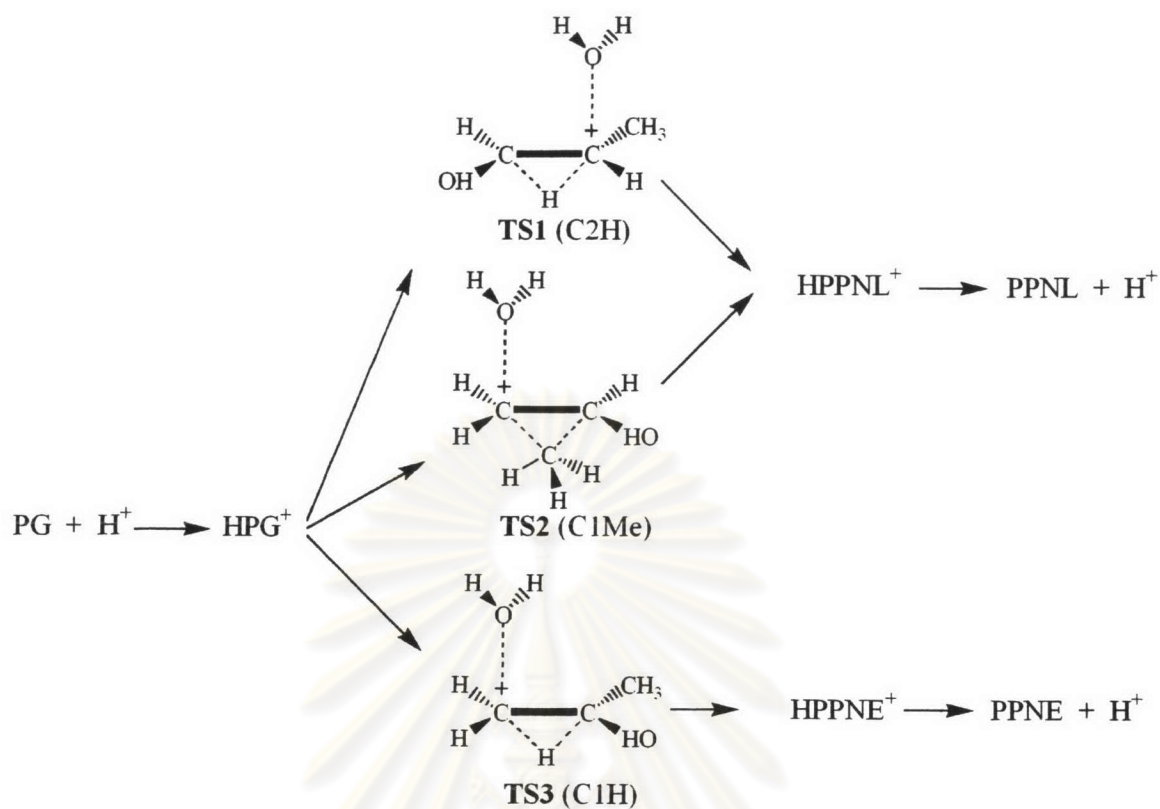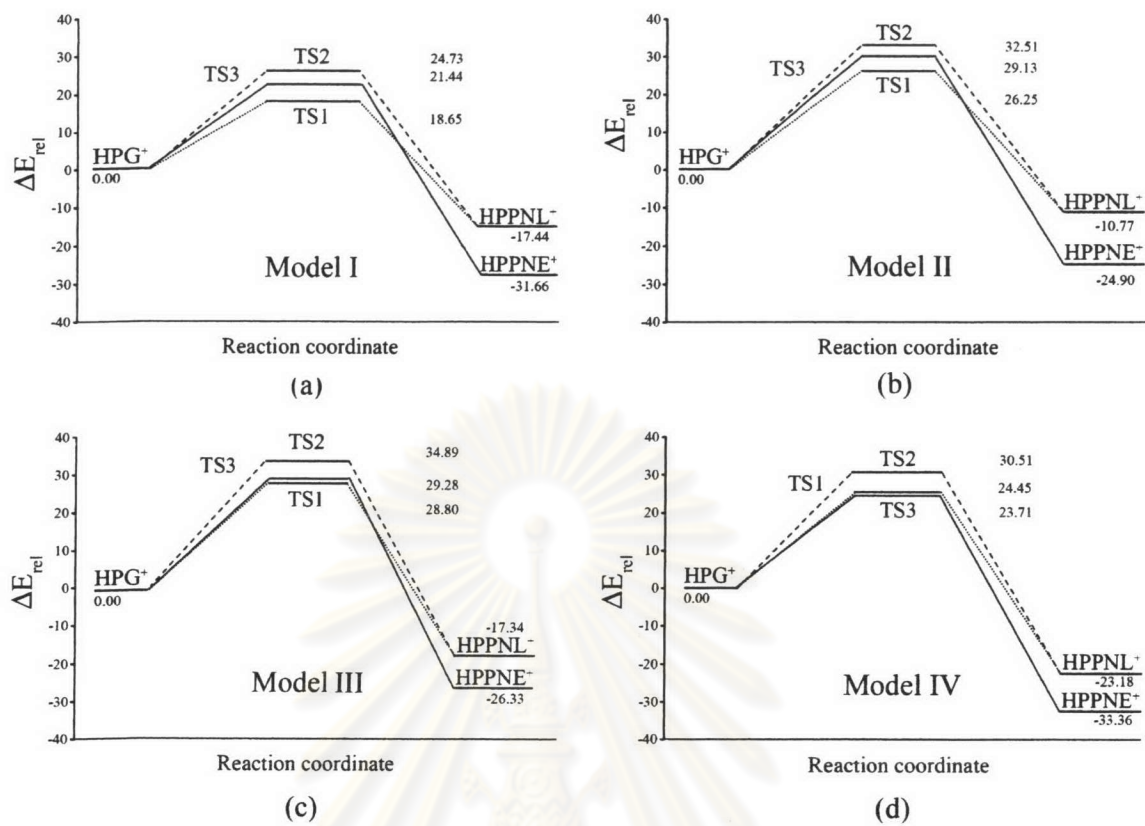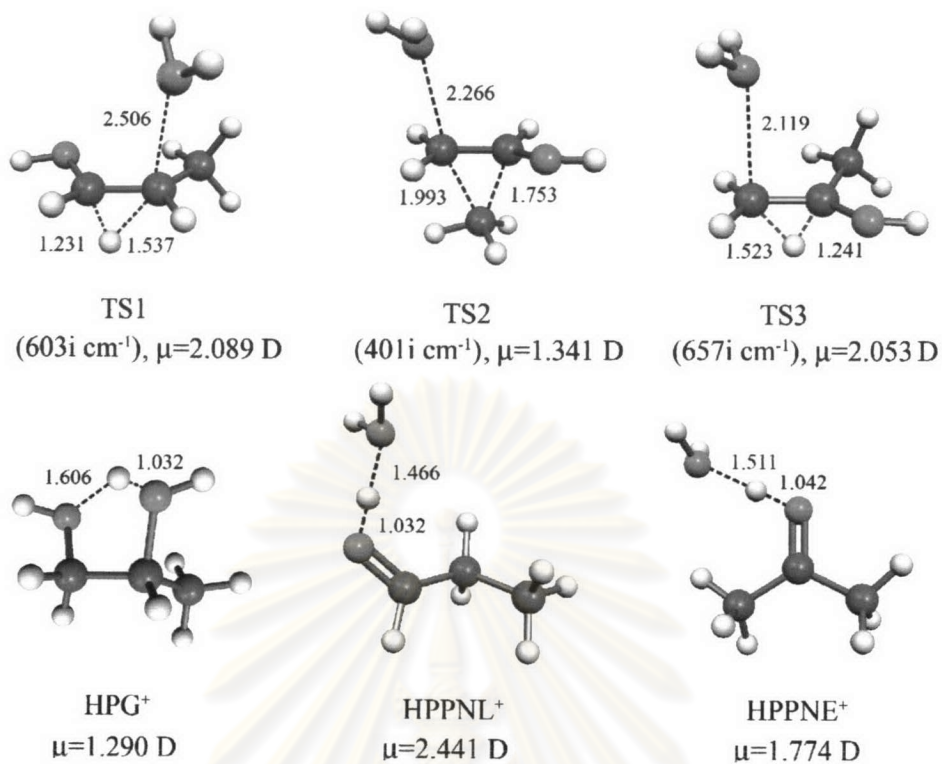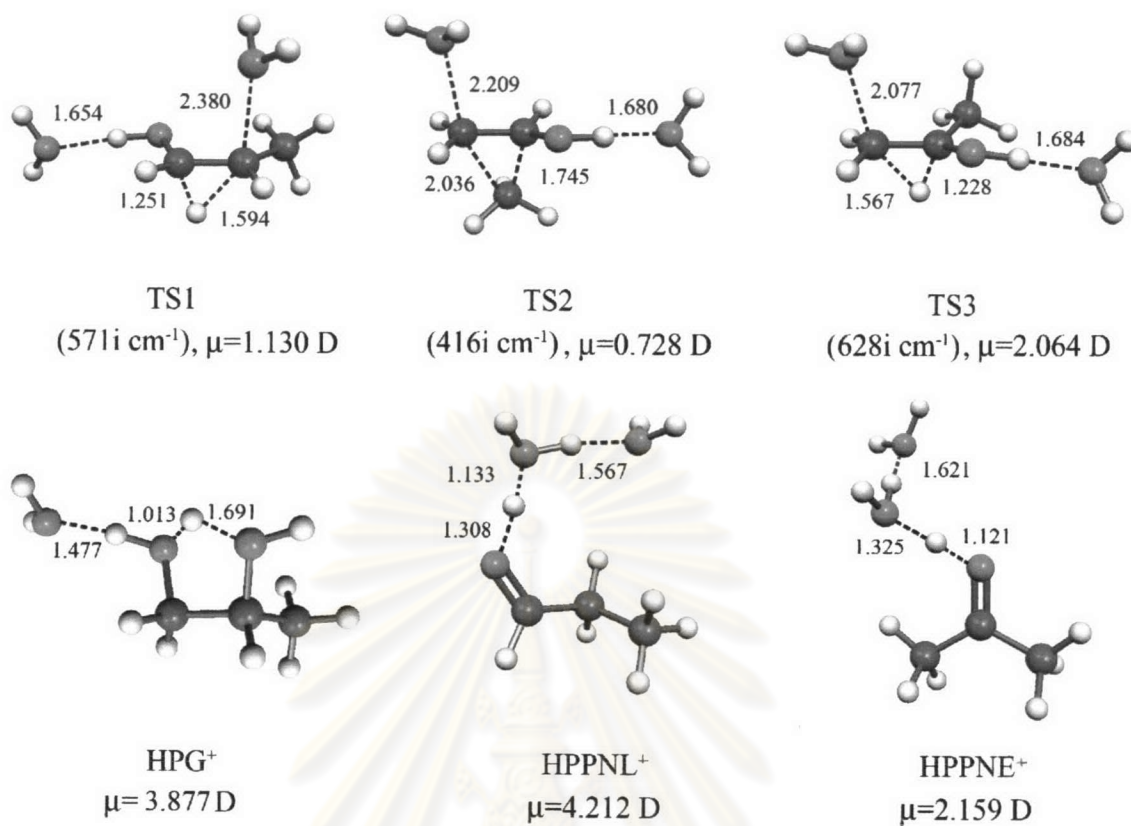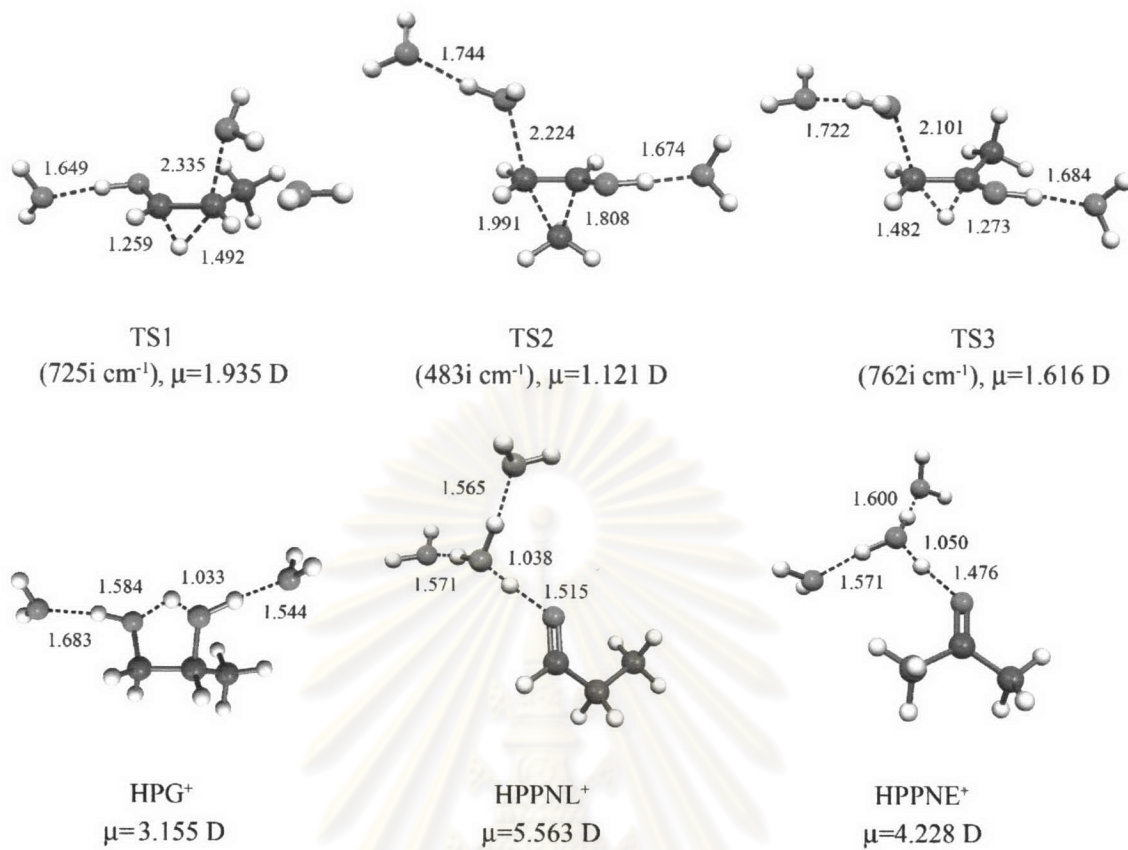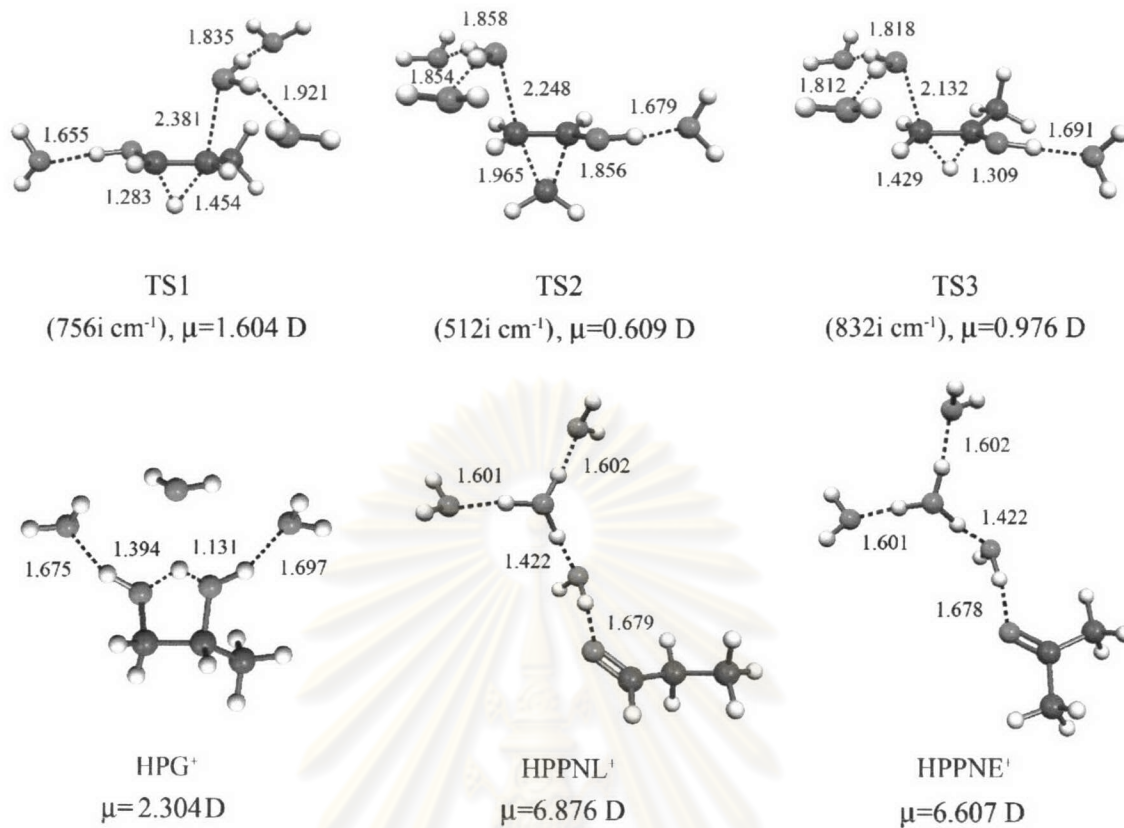
Figure 7.

VITA

NAME: Chompoonut   Rungnim

DATE AND PLACE OF BIRTH: 23 June 1981 in Bangkok, Thailand

ELEMENTARY SCHOOL:

1987-1991 Wattana Prueksa School, Nonthaburi

1991-1994 Wad Bow Nanthavithaya School, Nonthaburi

SECONDARY SCHOOL:

1994-1999 Suankularb Vithayalai Nonthaburi School, Nonthaburi

UNIVERSITY EDUCATION:

1999-2003 B. Sc. in Chemistry, Department of Chemistry, Faculty of Science

Chulalongkorn University, Bangkok

2003-2005 M. Sc. in Petrochemistry and Polymer Science, Faculty of Science,

Chulalongkorn University, Bangkok

PUBLICATION

C. Rungnim and V. Ruangpornvisuti "A Density Functional Study of Propylene Glycol Conversion to Propanal and Propanone of Various Acid-Catalyzed Reaction Models: A Water-Addition Effect" *J. Comput. Chem.* 26 (2005): 1592-1599.

PRESENTATION

C. Rungnim and V. Ruangpornvisuti "DFT Study on Reaction Mechanism of Dehydration of Propylene Glycol" in 30th Congress on Science and Technology of Thailand (STT 2004) on 19-24 October 2004 at Impact Exhibition and Convention Center, Thailand. (Poster)